

**Supporting Information to:**

**Amphiphilic block copolymers of mPEG-b-poly(MDO-co-vinyl esters) as a novel  
biodegradable nanocarrier platform**

Arunpandian Balaji<sup>a,b,c</sup>, Amber R. Prior<sup>a,b,c</sup>, Rachel K. O'Reilly<sup>d</sup>, Andrew P. Dove<sup>d</sup>, Kristofer J. Thurecht<sup>a,b,c</sup>,  
and Craig A. Bell<sup>a,b,c\*</sup>

<sup>a</sup> Centre for Advanced Imaging (CAI), The University of Queensland, Brisbane, QLD, Australia

<sup>b</sup> Australian Institute for Bioengineering & Nanotechnology (AIBN), The University of Queensland, Brisbane, QLD, Australia

<sup>c</sup> ARC Centre of Excellence for Convergent Bio-Nano Science & Technology, Monash University, Parkville, VIC, Australia

<sup>d</sup> School of Chemistry, University of Birmingham, Edgbaston, UK

\*Corresponding authors: [c.bell1@uq.edu.au](mailto:c.bell1@uq.edu.au)

**Contents**

Synthetic characterisation of mPEG-xanthate MacroCTA (3) .....	4
VBr polymer characterisation .....	9
VL polymer characterisation.....	21
Nanoparticle characterisation.....	28

### **Preparation of optical dye and cytotoxic drug incorporated hydrazone crosslinked micelles**

Cyanine 5 incorporated version of P4<sub>250</sub>, P5<sub>100</sub>, and P6<sub>100</sub> block copolymers were synthesized by following the previously established protocol<sup>1</sup>. The drug loading capability of these block copolymers were demonstrated by using a model drug, doxorubicin hydrochloride (DOX.HCl). Initially, to enable the loading into the hydrophobic core of the nanoparticles, the water soluble-hydrophilic DOX.HCl dissolved in DMSO was neutralised into free doxorubicin (DOX) by adding 3 molar excess of triethylamine and stirred overnight at room temperature. Then, to the above block copolymers dissolved in DMSO the DOX was added to make the final drug concentration of 10 wt% to the polymers taken. The block copolymers were self-assembled as described above, free DOX and unreacted catalyst was removed by dialysing (SnakeSkin™ Dialysis Tubing, 10K MWCO) against Milli-Q water for 48 h with the dialysing media being changed every 12 h.

### **Preparation of optical dye and cytotoxic drug incorporated SPAAC crosslinked micelles**

To enable loading into the hydrophobic core of the nanoparticles, the water soluble-hydrophilic DOX.HCl was dissolved in DMF and neutralised with 3 molar excess of triethylamine and stirred overnight at room temperature. Then, the above block copolymers (10 mg each) were dissolved in the DOX/DMF solution to make a final drug concentration of 10 wt% to the polymers at a polymer concentration of 10 mg/mL. To each of these solutions, Cy5-DBCO (2.4 µL @ 50 mg/mL in DMF) was added, and these were then stirred in the dark at RT for an additional 24 h. The block copolymers were then self-assembled by solvent switch incorporation of Milli-Q water at a rate of 0.6 ml/h. After full addition of water, a solution of DBCO-PEG<sub>4</sub>-DBCO in DMF (0.5 mol equivalents to azide units) was added at high stirring (1000 RPM), and again the solutions were stirred for 24 h to ensure complete crosslinking. Finally, free DOX and unreacted crosslinker was removed by dialysing (SnakeSkin™ Dialysis Tubing, 10K MWCO) against Milli-Q water for 48 h with the dialysing media being changed every 12 h.

### **Hemolysis assays**

To measure the haemolysis percentage of the nanoassemblies, the whole blood was collected from Balb/c nude mice in EDTA coated tubes and centrifuged at 3000 rpm for 4 min to separate the plasma. Then, the erythrocyte portion was washed with PBS (pH 7.4) twice at the above setting, and the supernatant was discarded. Finally, the blood cells were diluted to the initial volume by adding fresh PBS. To prepare the assay mixture, the micelles solution (in PBS) and the blood cell suspension was mixed in equal volume (1:1, 0.6 mg/mL final polymer concentration). Further, the blood cells and distilled water mixture (1:1) was considered a positive control, whilst the PBS and whole blood mixture were taken as a negative control. All samples were shifted to a shaking incubator at 100 rpm and maintained at 37 °C. After 1 h, the samples were centrifuged at

3500 rpm for 4 min, and the OD value of the supernatant was measured at 540 nm using a Tecan plate reader. Finally, the haemolysis percentage (HP) was calculated using the following formula:

$$\text{HP (\%)} = [(\text{OD test sample} - \text{OD negative control}) / (\text{OD positive control} - \text{OD negative control})] \times 100$$

## Synthetic characterisation of mPEG-xanthate MacroCTA (3)

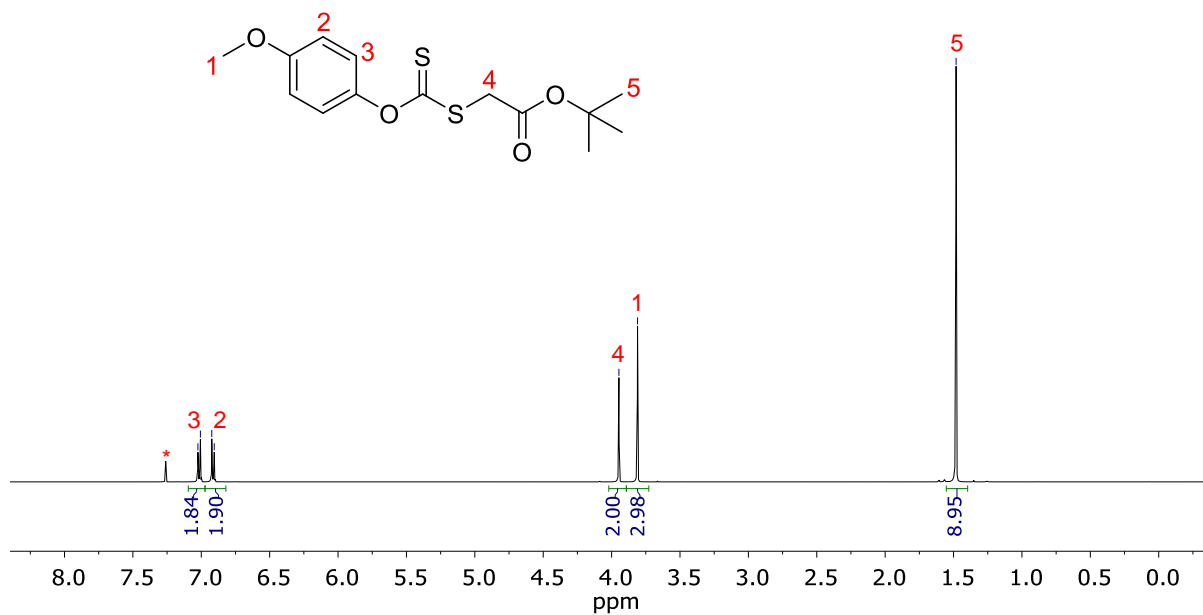


Figure S1 – <sup>1</sup>H NMR (CDCl<sub>3</sub>, 500 MHz) spectrum of 1. \* - residual CHCl<sub>3</sub>.

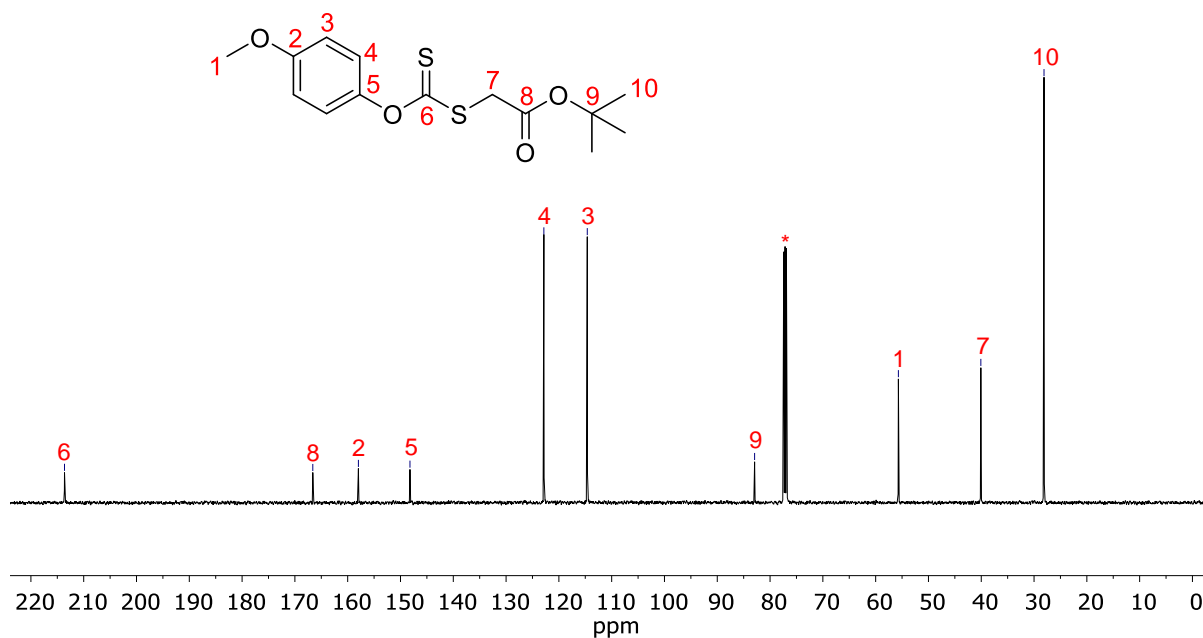
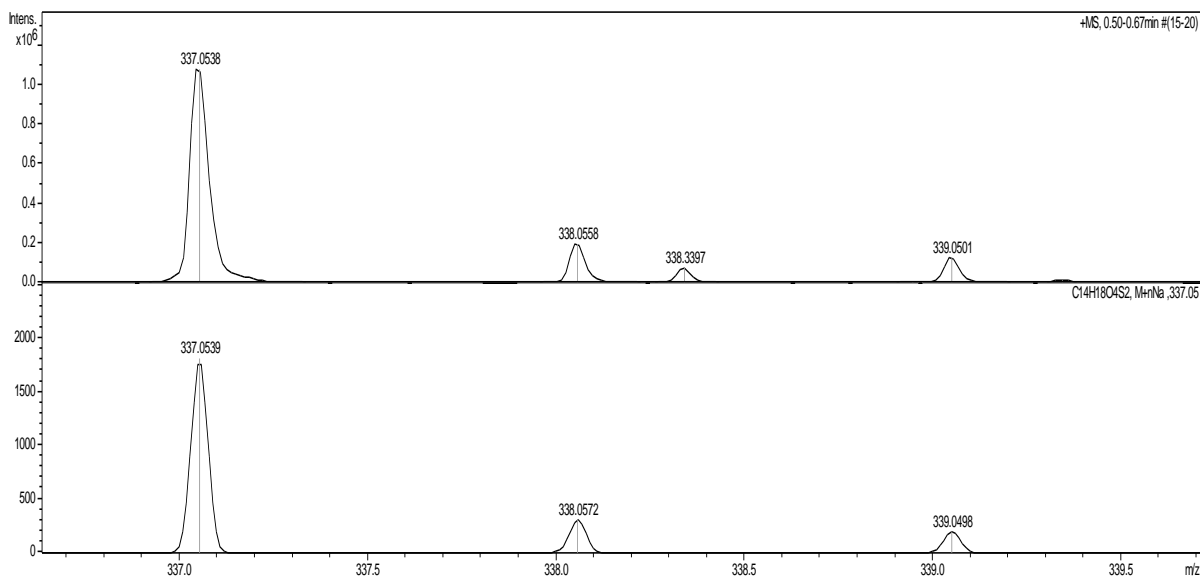
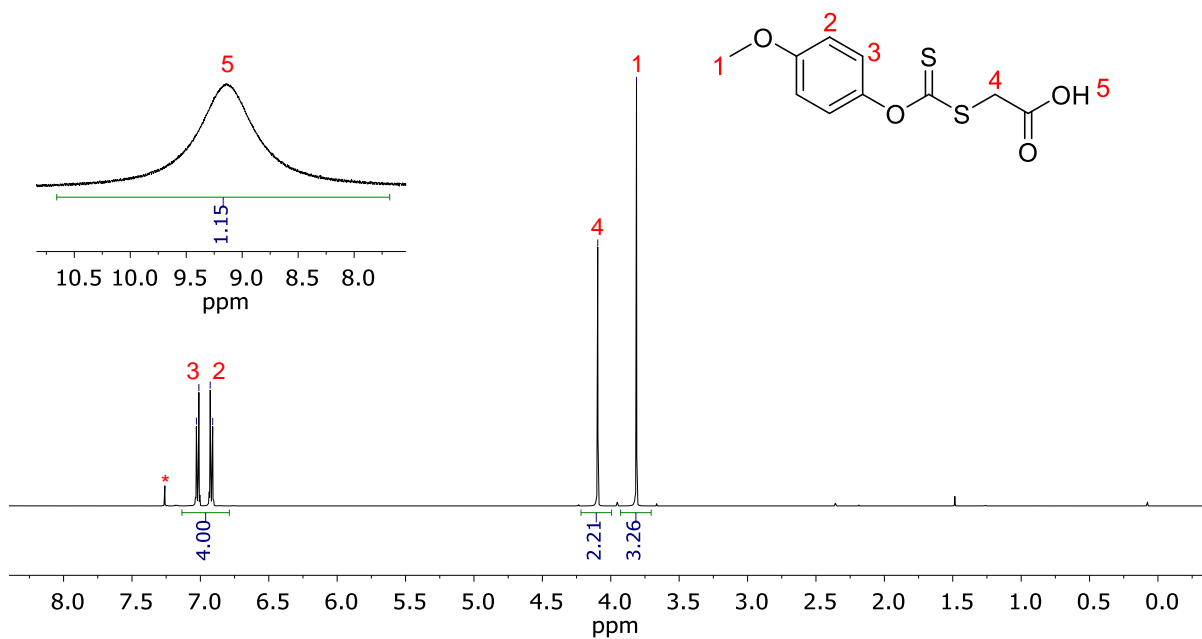


Figure S2 – <sup>13</sup>C NMR (CDCl<sub>3</sub>, 125 MHz) spectrum of 1. \* - residual CHCl<sub>3</sub>.



**Figure S3** – HRMS spectrum of **1**. Top – experimental; bottom – simulated with formula  $C_{14}H_{18}O_4S_2Na^+$  = 337.0539.



**Figure S4** –  $^1H$  NMR ( $CDCl_3$ , 500 MHz) spectrum of **2**. \* - residual  $CHCl_3$ .

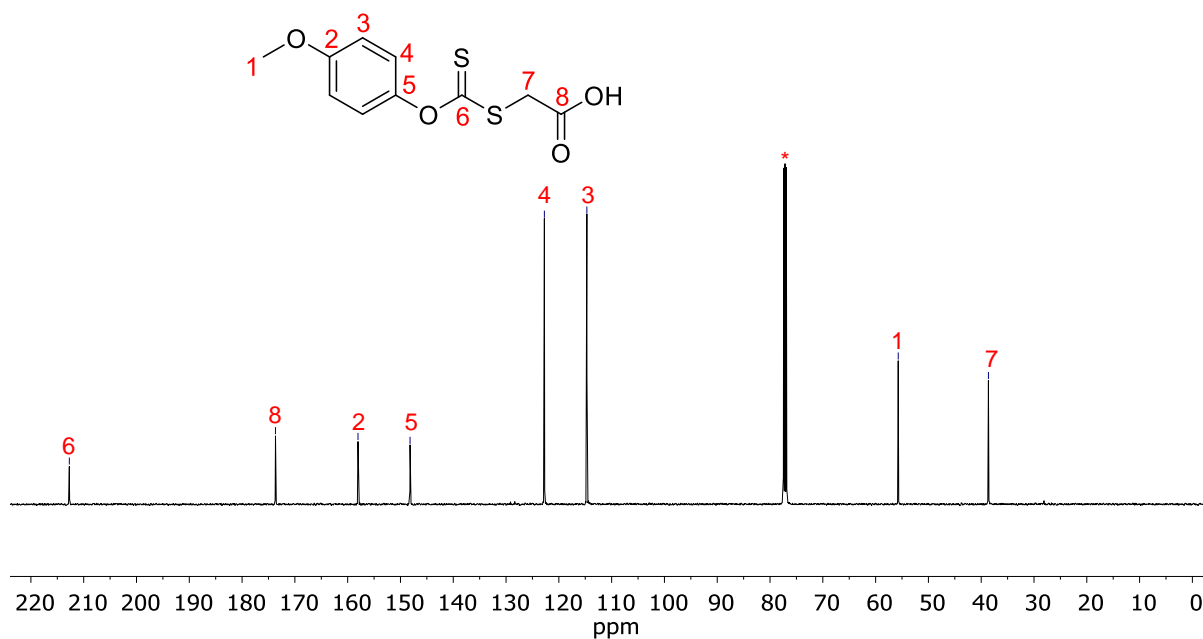


**Figure S5** –  $^{13}\text{C}$  NMR ( $\text{CDCl}_3$ , 125 MHz) spectrum of **2**. \* - residual  $\text{CHCl}_3$ .

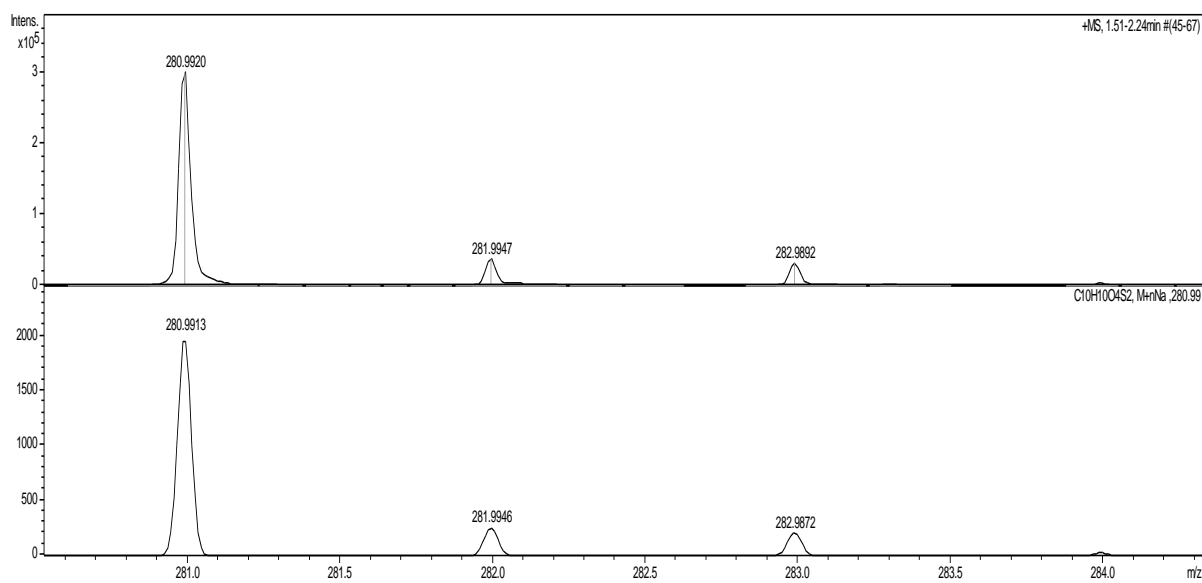


**Figure S6** – HRMS spectrum of **2**. Top – experimental; bottom – simulated with formula  $\text{C}_{10}\text{H}_{10}\text{O}_4\text{S}_2\text{Na}^+ = 280.9913$ .

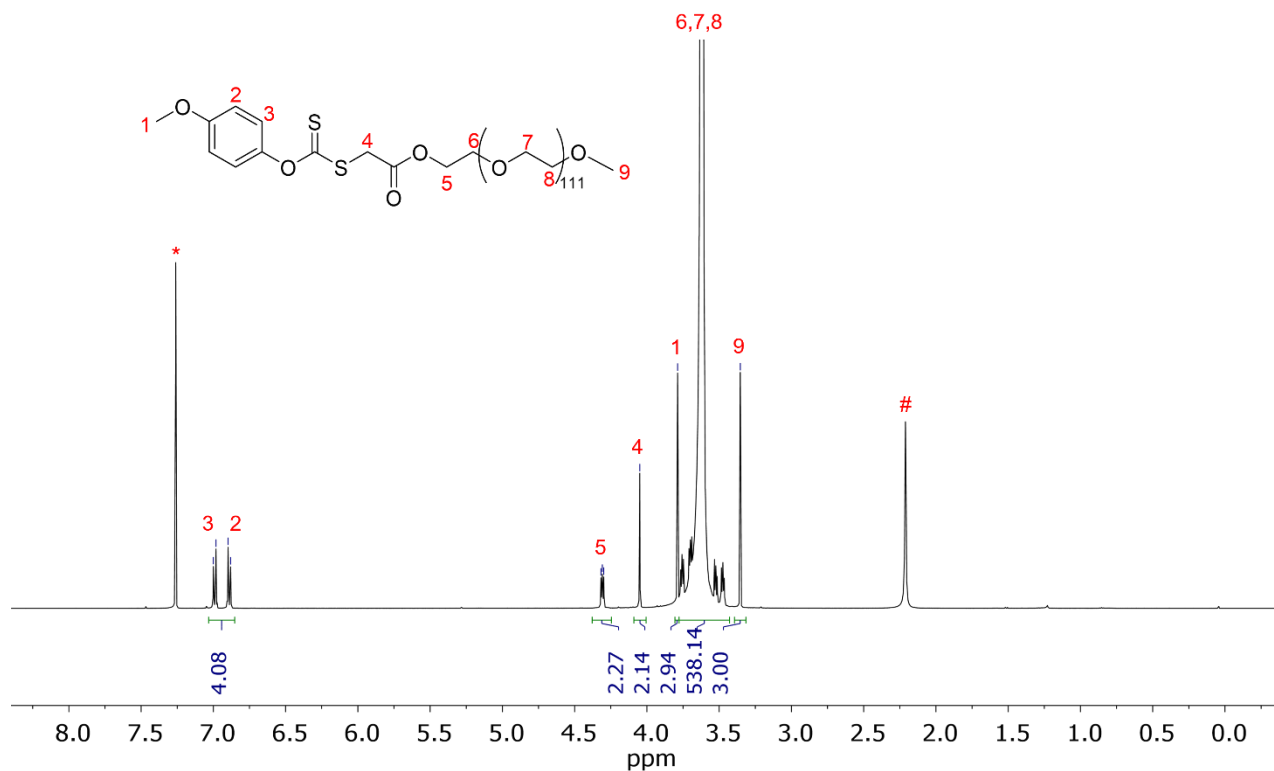


**Figure S7** –  $^1\text{H}$  NMR ( $\text{CDCl}_3$ , 500 MHz) spectrum of **3**. \* - residual  $\text{CHCl}_3$ ; # -  $\text{H}_2\text{O}$ .

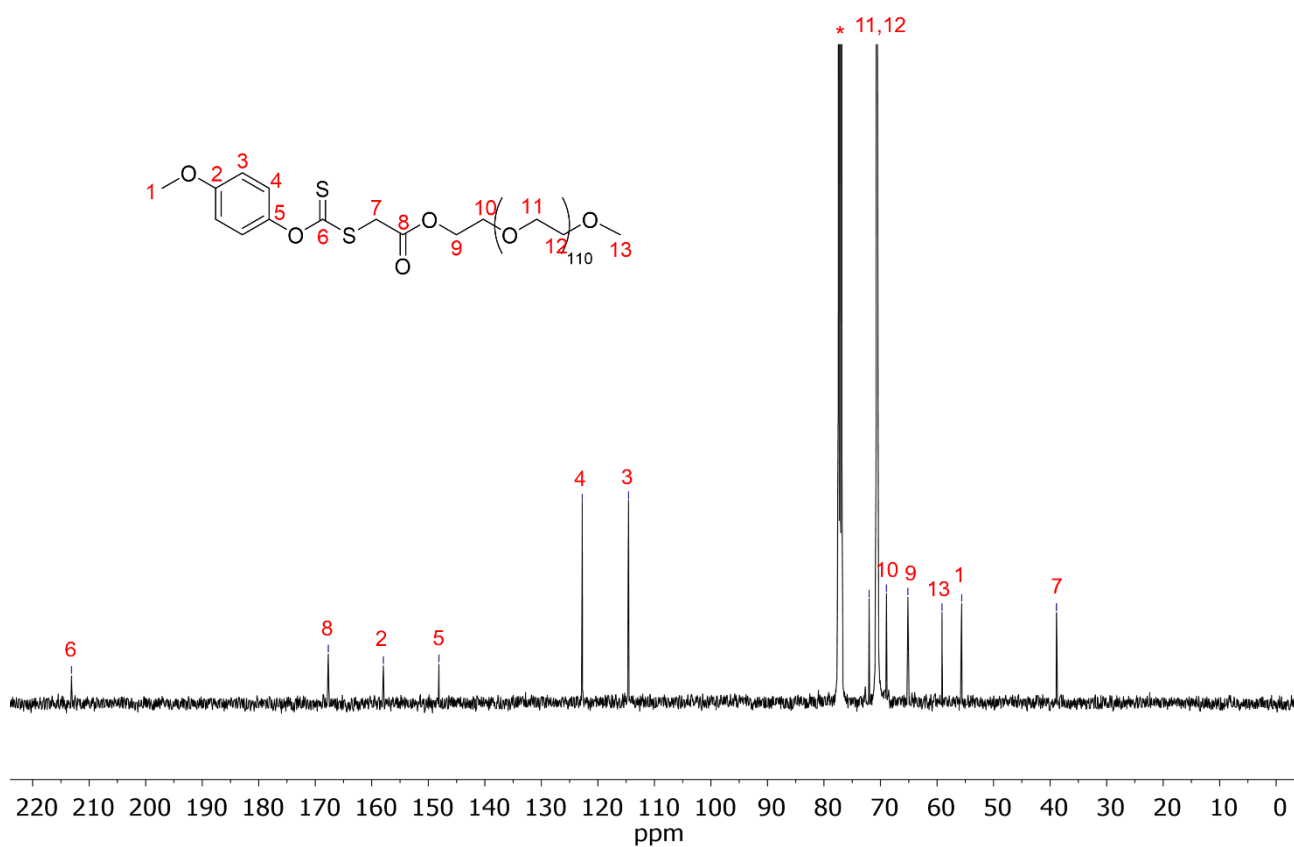


**Figure S8** –  $^{13}\text{C}$  NMR ( $\text{CDCl}_3$ , 125 MHz) spectrum of **3**. \* - residual  $\text{CHCl}_3$ .

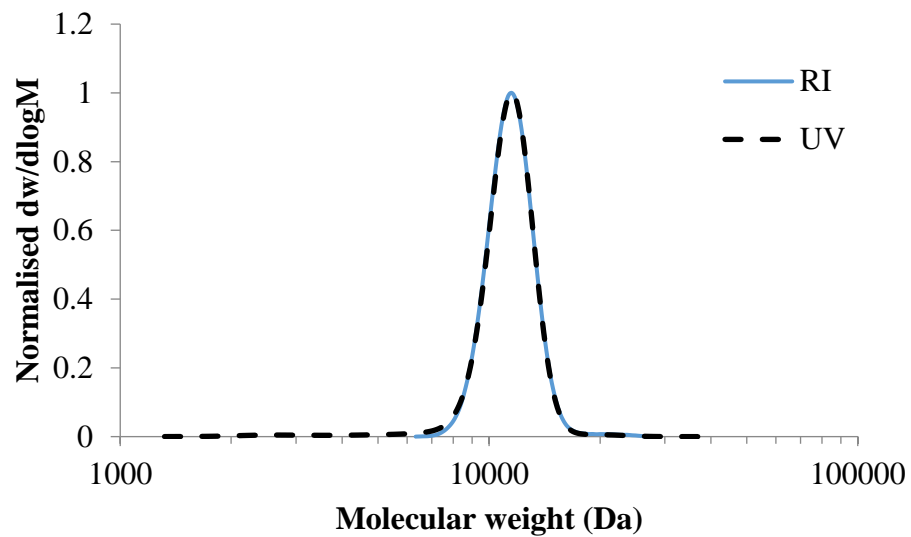


**Figure S9** – SEC (DMF + 5 mM  $\text{NH}_4\text{BF}_4$ ) chromatograms of **3**. Dashed line indicates the UV detector trace at 280 nm.



## VBr polymer characterisation

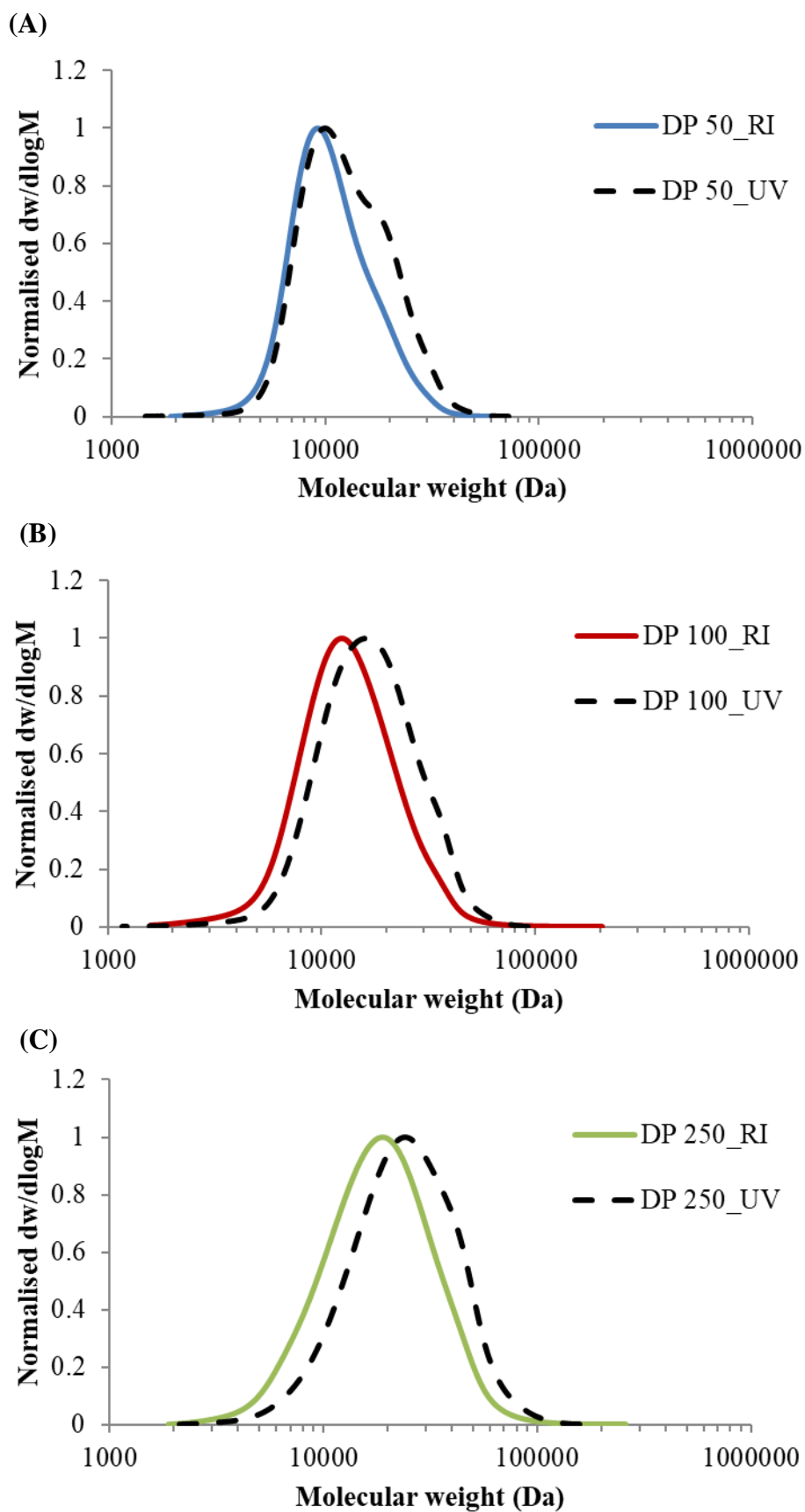


**Figure S10** – GPC chromatograms for the copolymerisation of VAc, VBr, and MDO with **3** (entries 1-3 in Table 1). (A) **P1<sub>50</sub>**, (B) **P1<sub>100</sub>** and (C) **P1<sub>250</sub>**. All chromatograms are normalised to peak height and the dashed line indicates the UV detector trace at 280 nm.

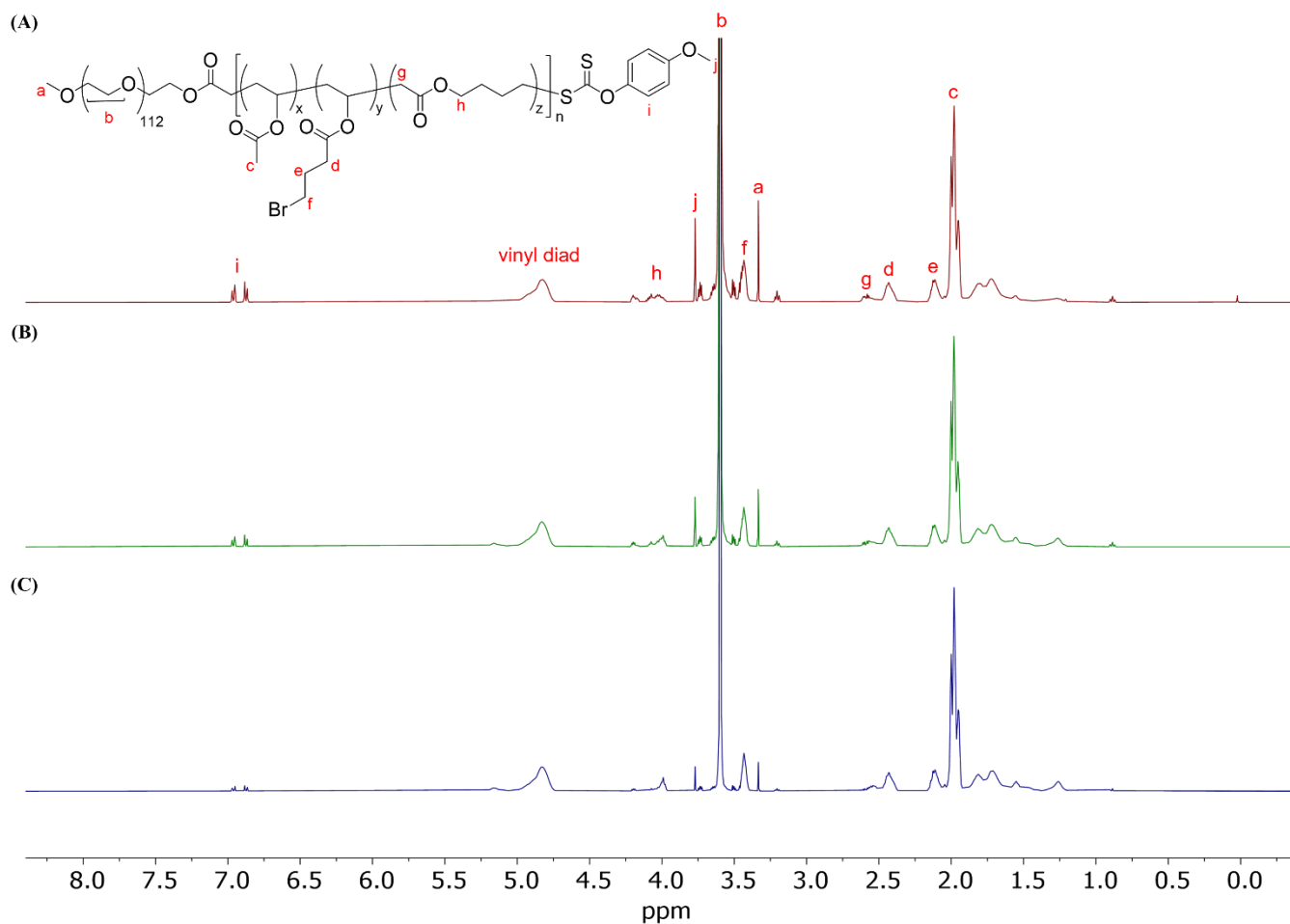


**Figure S11** – <sup>1</sup>H NMR spectra for the copolymerisation of VAc, VBr, and MDO with **3** (entries 1-3 in Table 1). (A) **P150**, (B) **P1100** and (C) **P1250**

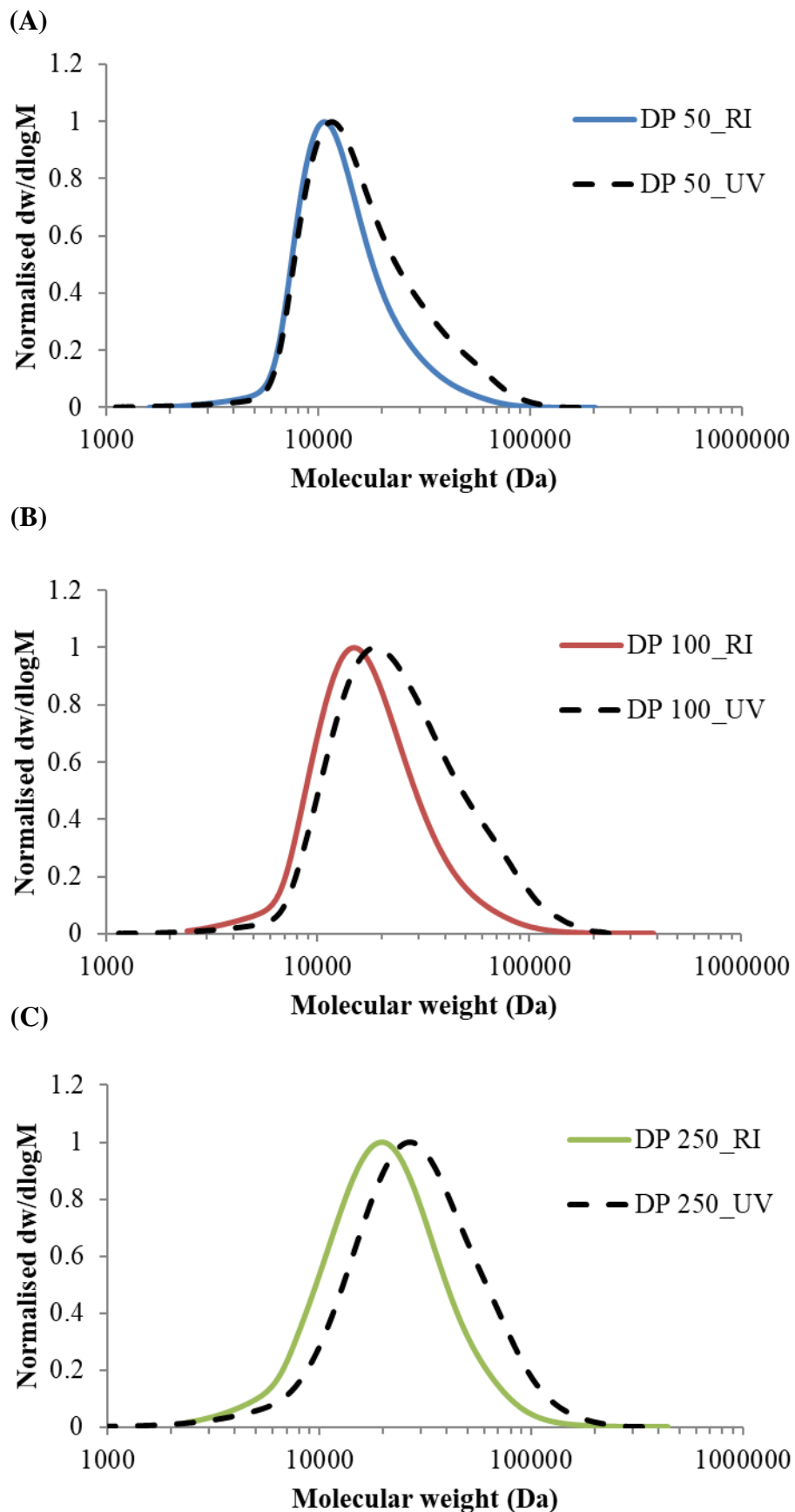


**Figure S12** – GPC chromatograms for the copolymerisation of VAc, VBr, and MDO with **3** (entries 4-6 in Table 1). (A) **P250**, (B) **P100** and (C) **P250**. All chromatograms are normalised to peak height and the dashed line indicates the UV detector trace at 280 nm.

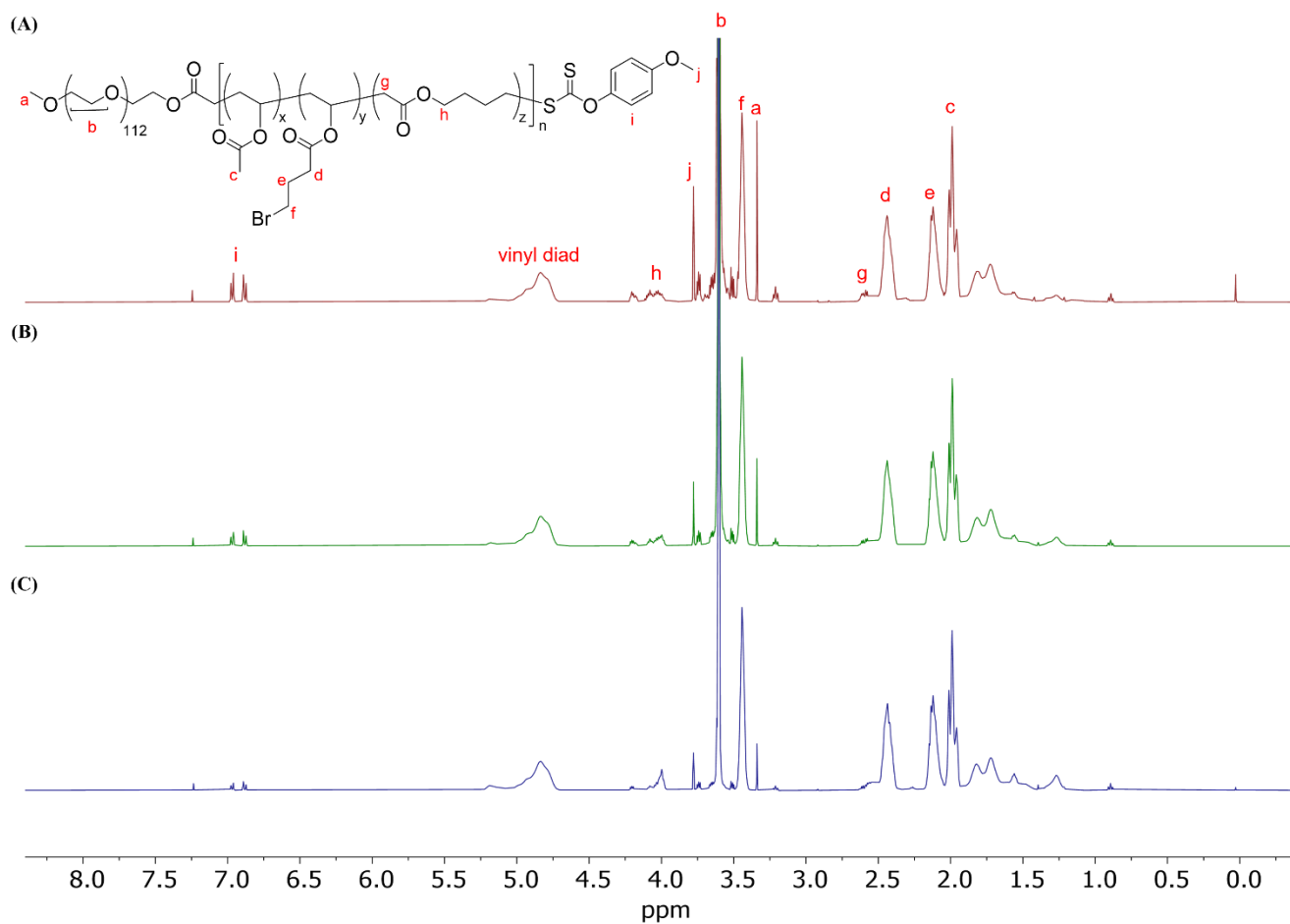


**Figure S13** –  $^1\text{H}$  NMR spectra for the copolymerisation of VAc, VBr, and MDO with **3** (entries 4-6 in Table 1). (A) **P250**, (B) **P2100** and (C) **P2250**

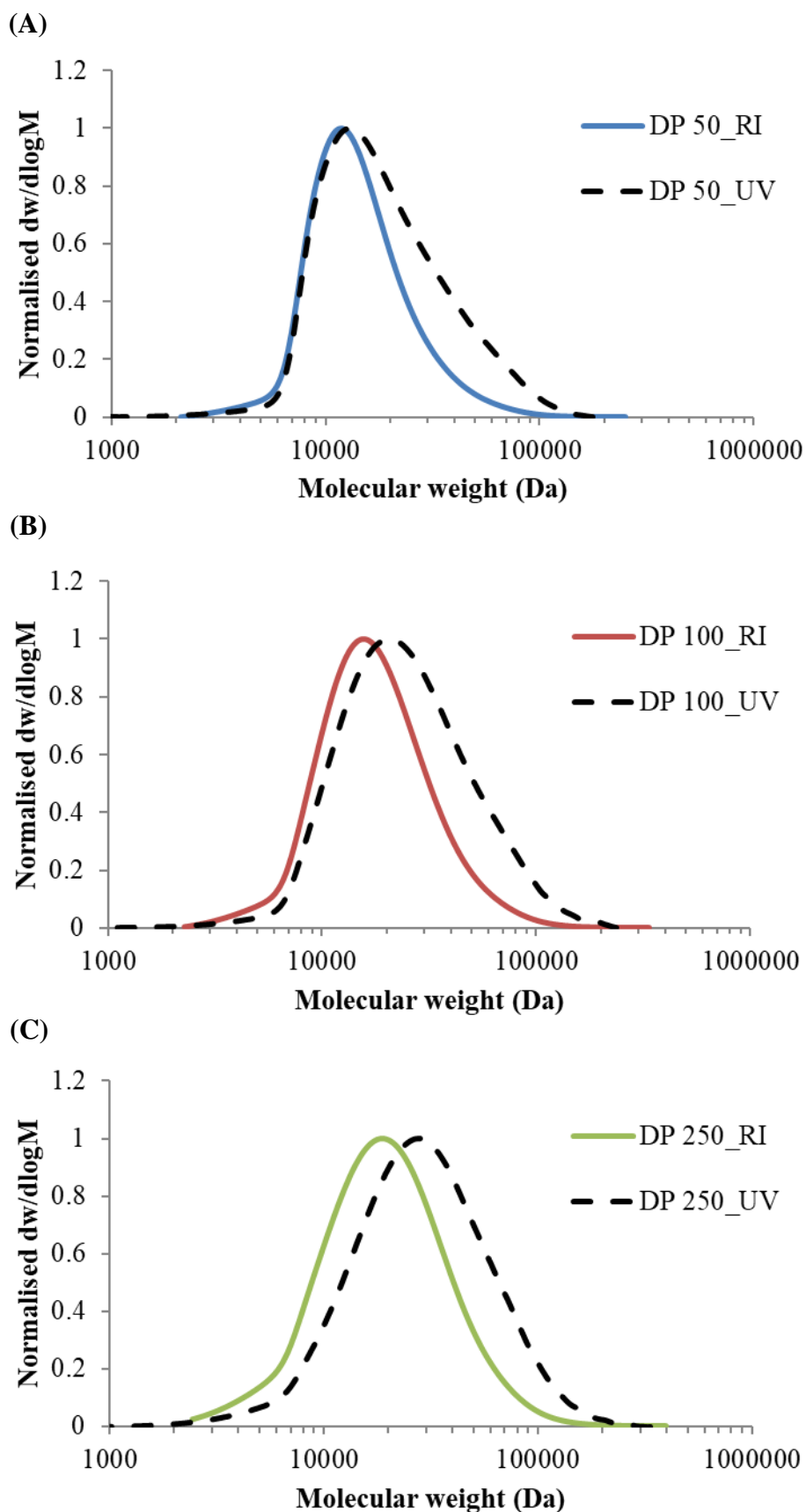


**Figure S14** – GPC chromatograms for the copolymerisation of VAc, VBr, and MDO with **3** (entries 7-9 in Table 1). (A) **P3<sub>50</sub>**, (B) **P3<sub>100</sub>** and (C) **P3<sub>250</sub>**. All chromatograms are normalised to peak height and the dashed line indicates the UV detector trace at 280 nm.

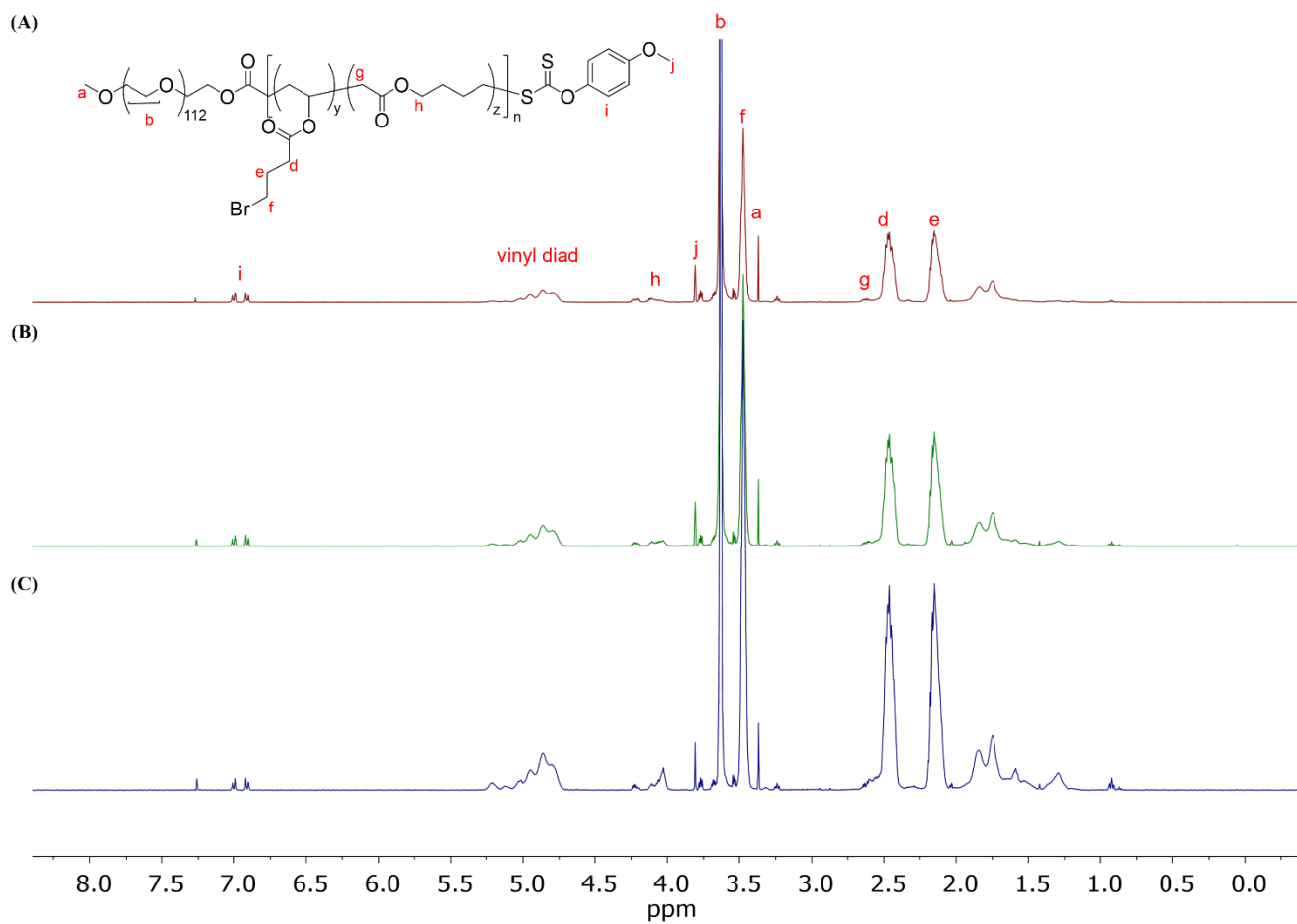


**Figure S15** –  $^1\text{H}$  NMR spectra for the copolymerisation of VAc, VBr, and MDO with **3** (entries 7-9 in Table 1). (A) **P3<sub>50</sub>**, (B) **P3<sub>100</sub>** and (C) **P3<sub>250</sub>**

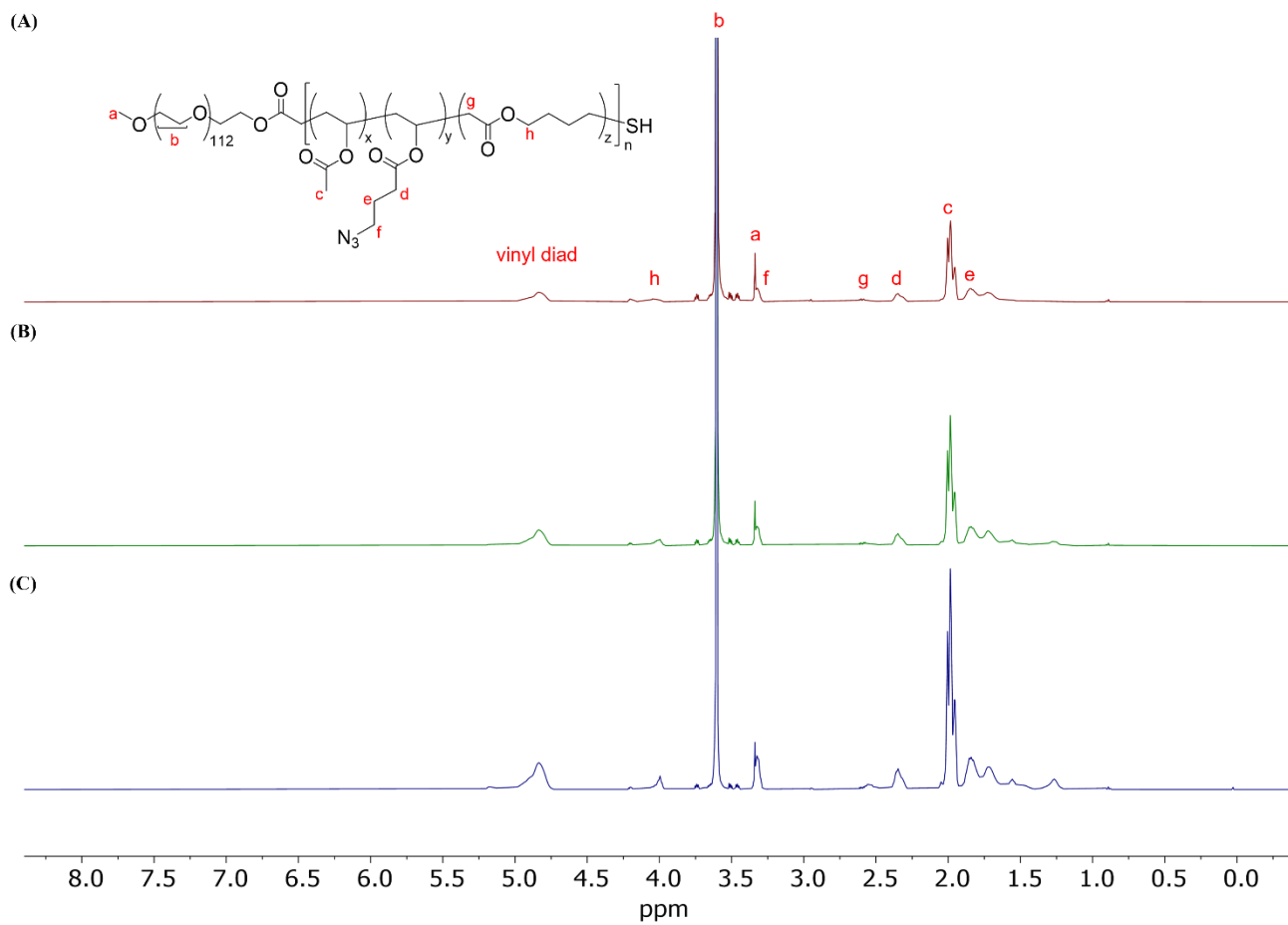


**Figure S16** –  $^1\text{H}$  NMR spectra after azidation of the Br containing block copolymers. (A) **P1Az50**, (B) **P1Az100** and (C) **P1Az250**

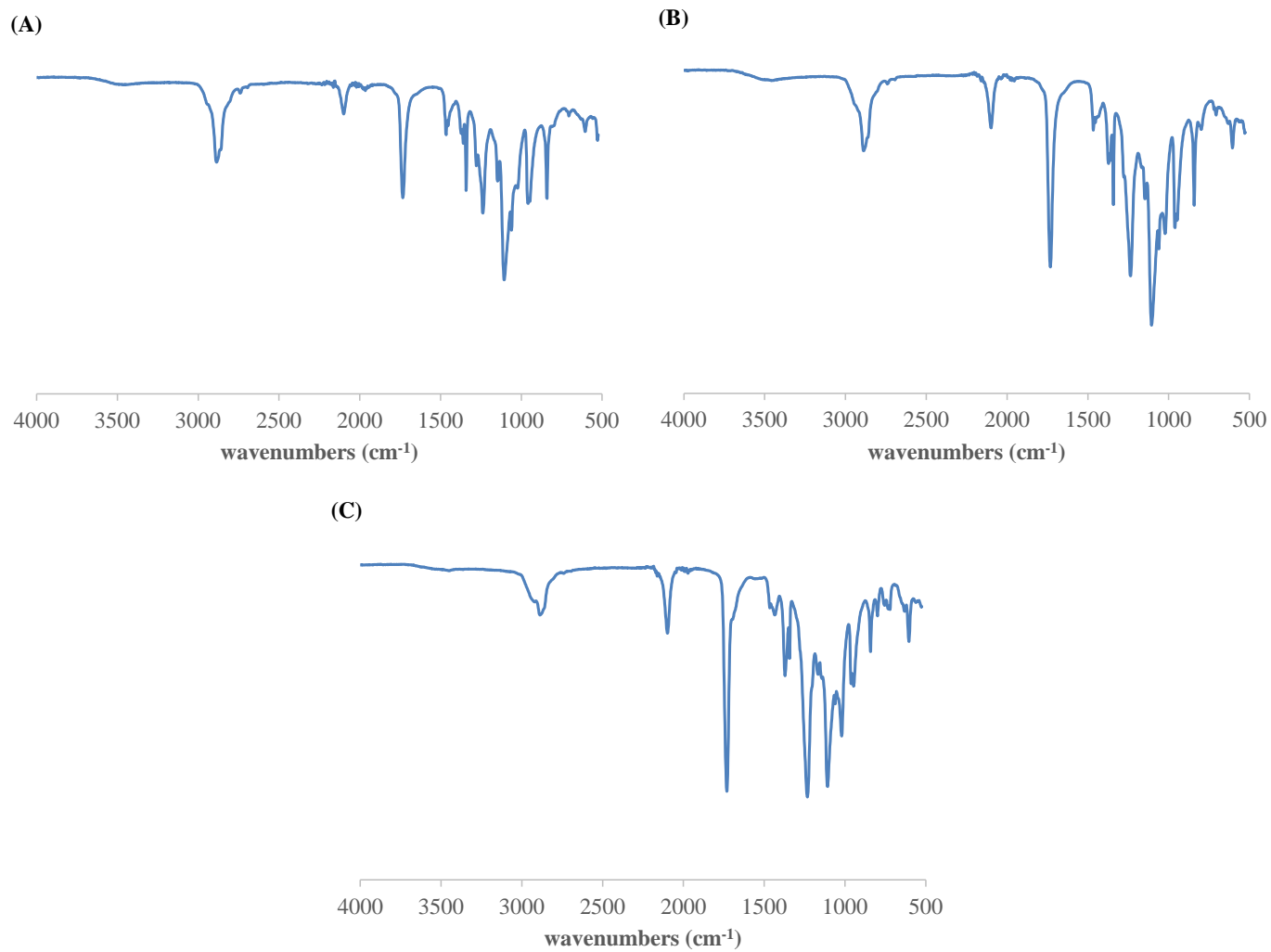


**Figure S17** – ATR-FTIR spectra of (A) **P1Az50**, (B) **P1Az100** and (C) **P1Az250**



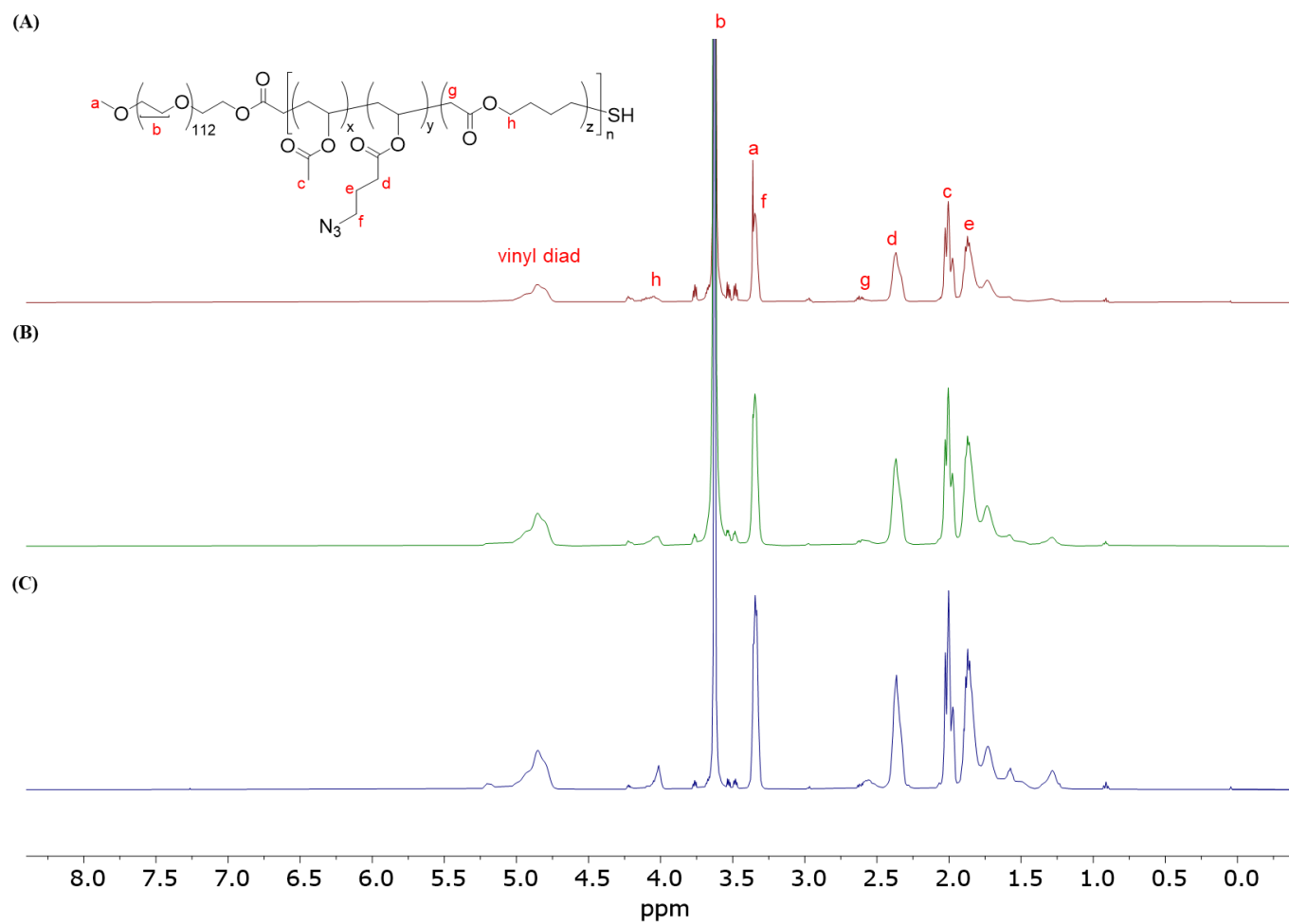


**Figure S18** – <sup>1</sup>H NMR spectra after azidation of the Br containing block copolymers. (A) **P2Az<sub>50</sub>**, (B) **P2Az<sub>100</sub>** and (C) **P2Az<sub>250</sub>**

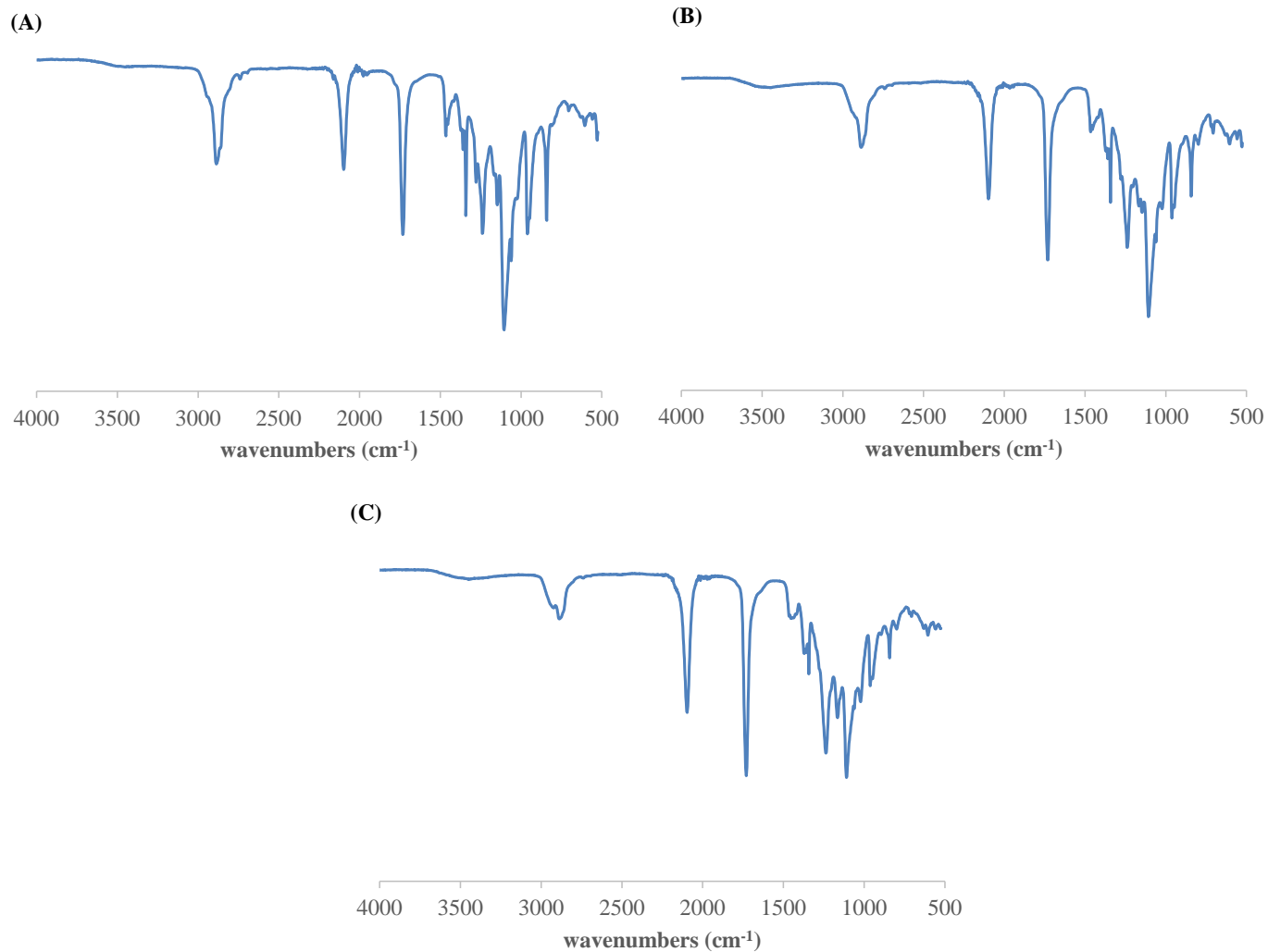


**Figure S19** – ATR-FTIR spectra of (A) **P2Az<sub>50</sub>**, (B) **P2Az<sub>100</sub>** and (C) **P2Az<sub>250</sub>**

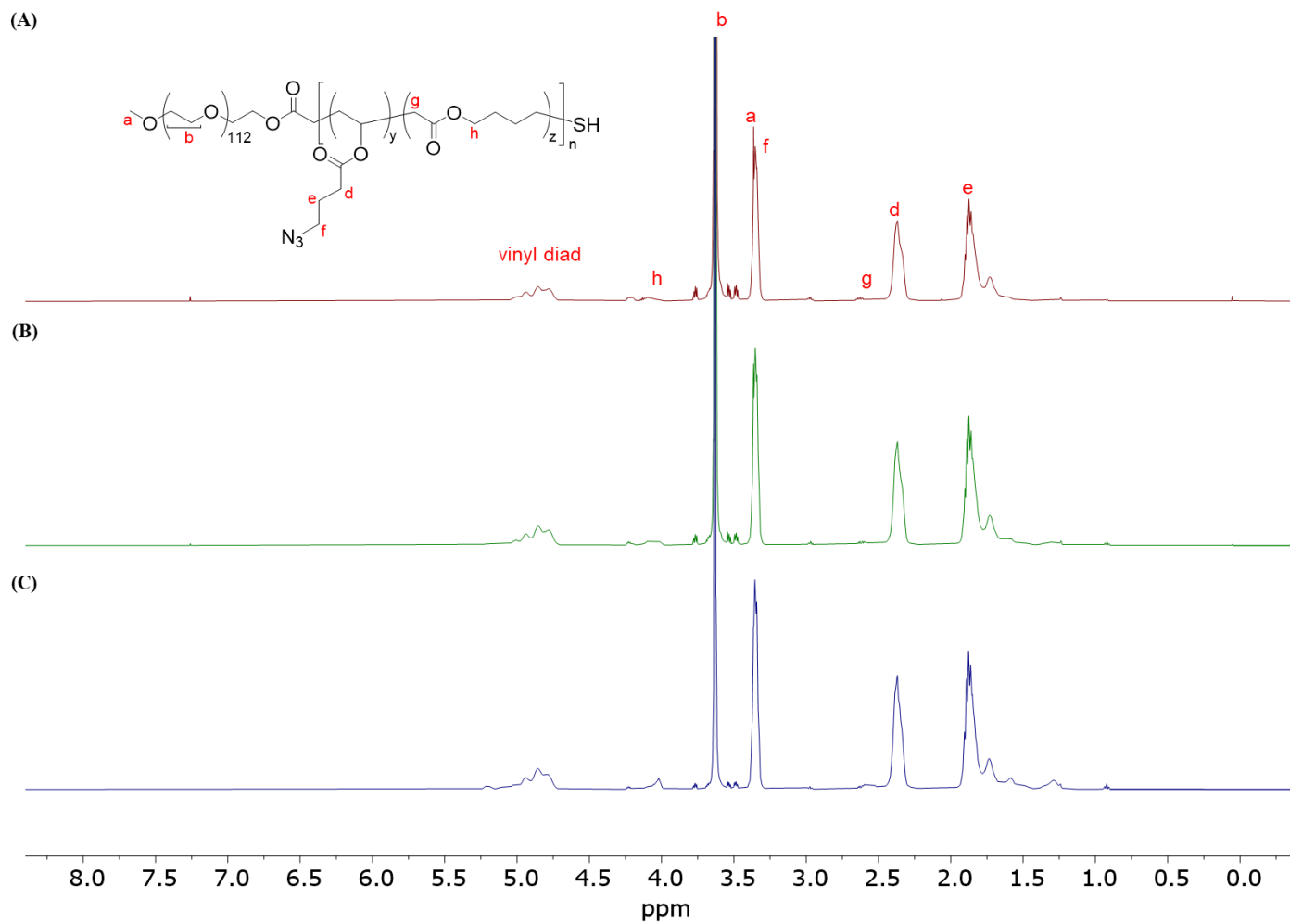


**Figure S20** –  $^1\text{H}$  NMR spectra after azidation of the Br containing block copolymers. (A) **P3Az<sub>50</sub>**, (B) **P3Az<sub>100</sub>** and (C) **P3Az<sub>250</sub>**

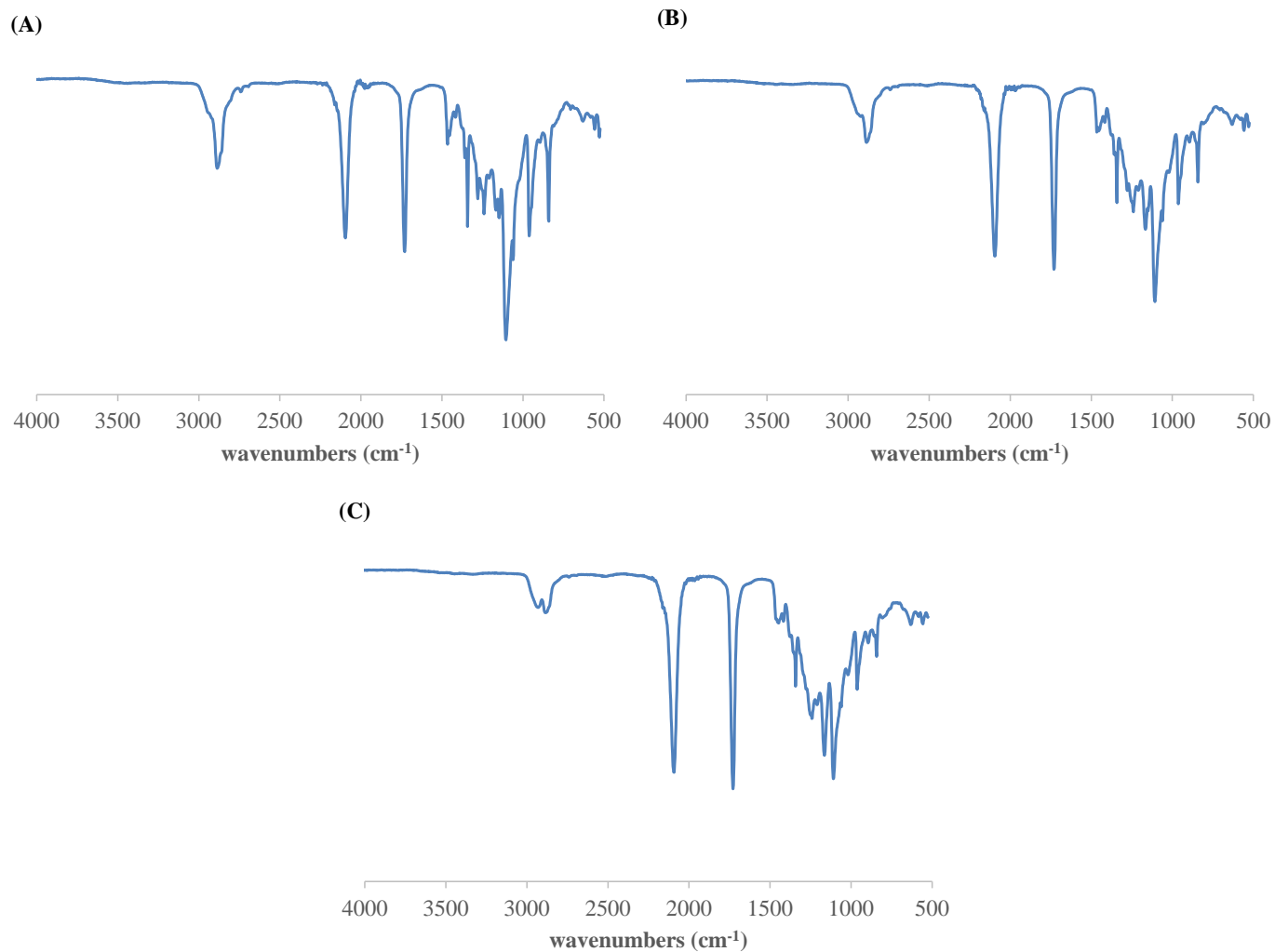


**Figure S21** – ATR-FTIR spectra of (A) **P3Az<sub>50</sub>**, (B) **P3Az<sub>100</sub>** and (C) **P3Az<sub>250</sub>**

## VL polymer characterisation

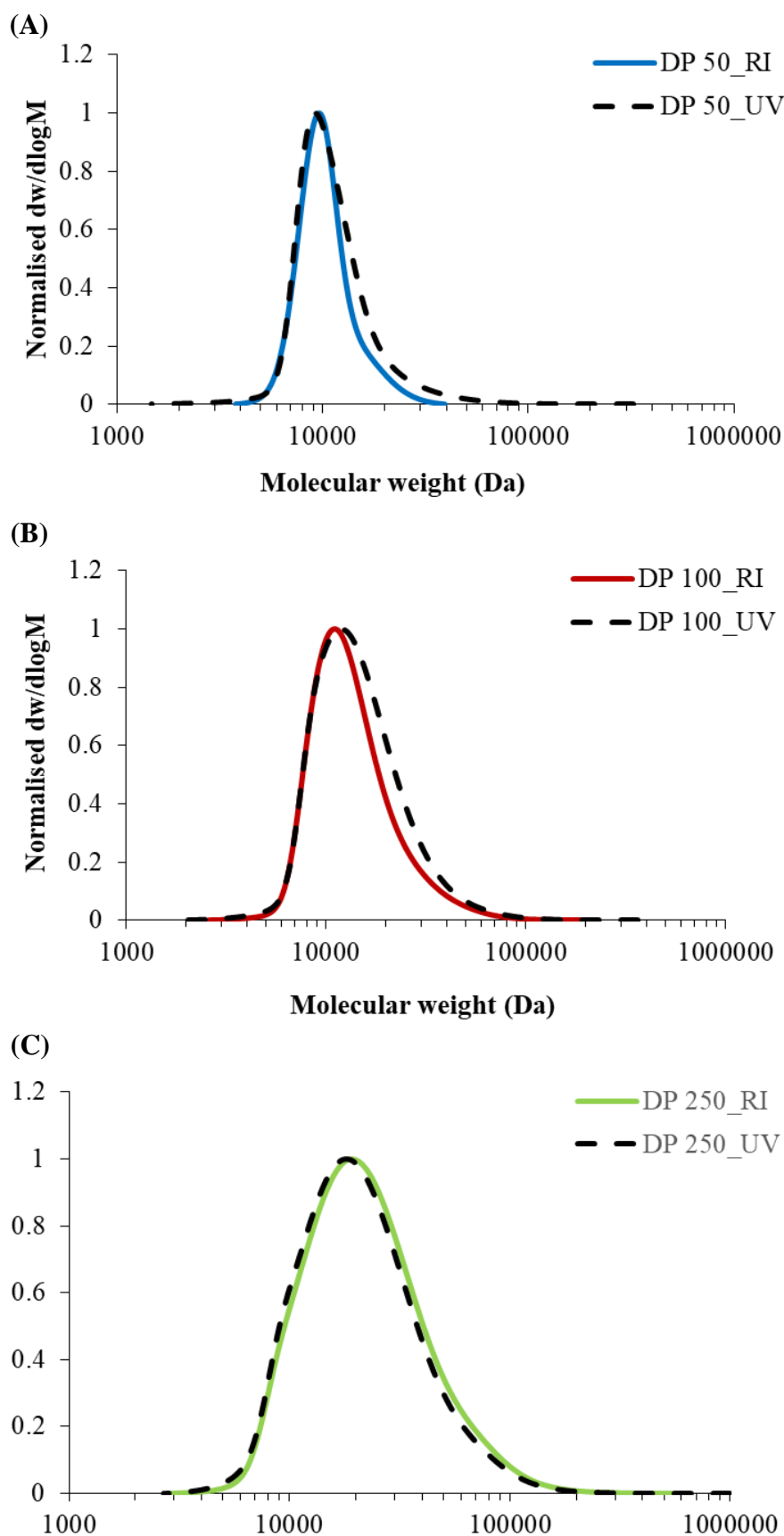


**Figure S22** – GPC chromatograms for the copolymerisation of VAc, VL, and MDO with **3** (entries 1-3 in Table 2). (A) **P4<sub>50</sub>**, (B) **P4<sub>100</sub>** and (C) **P4<sub>250</sub>**. All chromatograms are normalised to peak height and the dashed line indicates the UV detector trace at 280 nm.

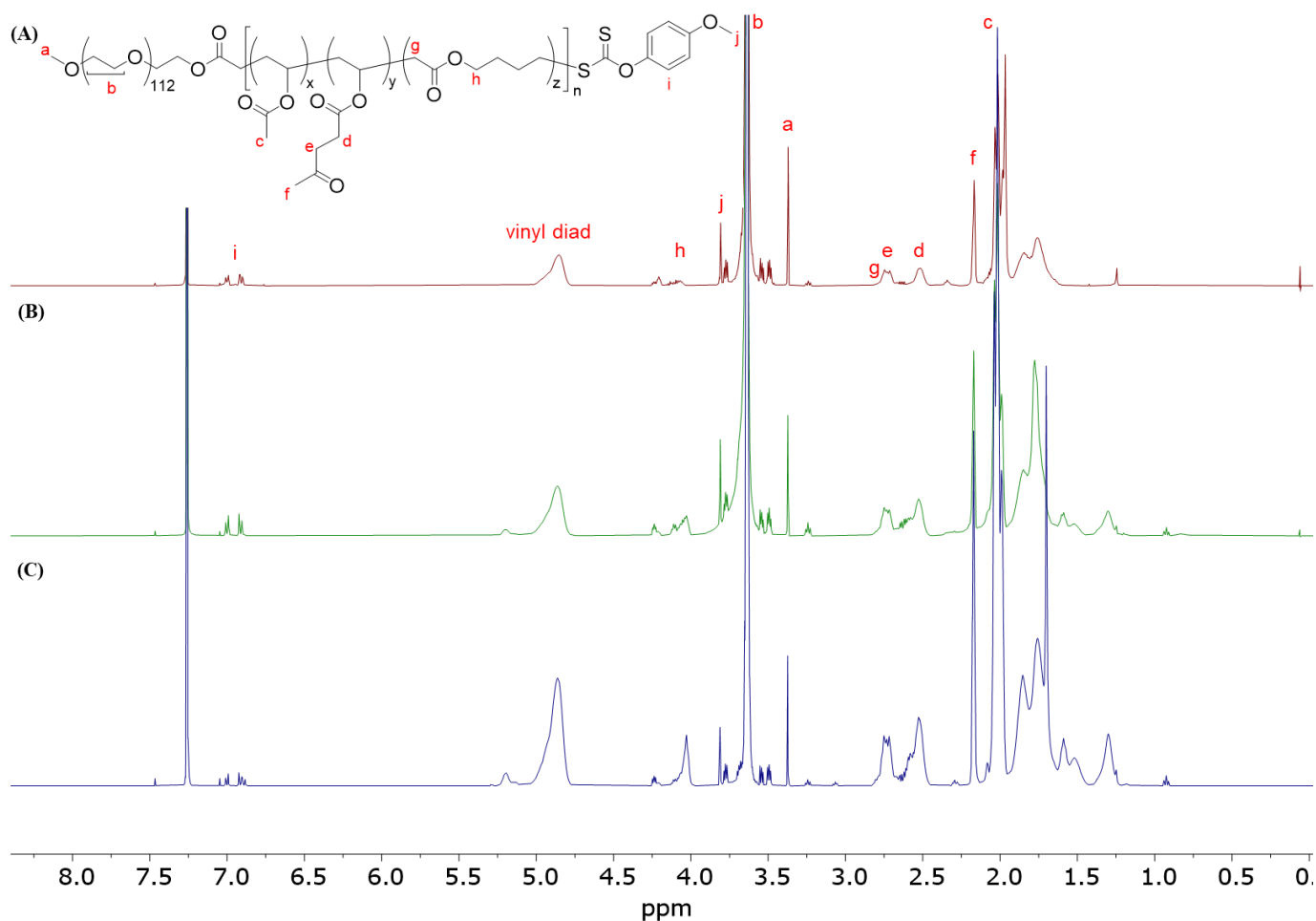


**Figure S23** –  $^1\text{H}$  NMR spectra for the copolymerisation of VAc, VL, and MDO with **3** (entries 1-3 in Table 2). All spectrum intensities are normalised to the PEG signal at 3.6 ppm. (A) **P4<sub>50</sub>**, (B) **P4<sub>100</sub>** and (C) **P4<sub>250</sub>**

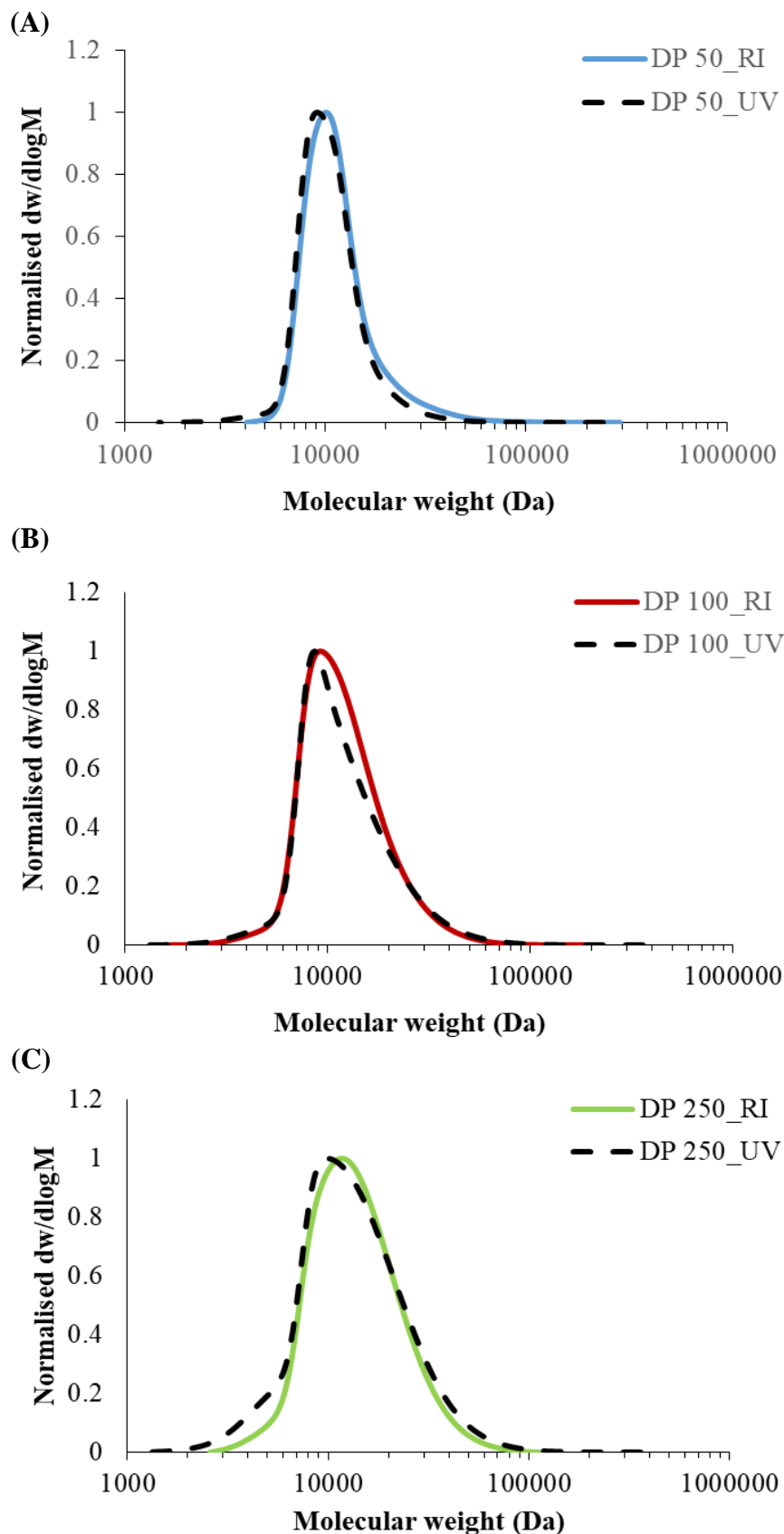


**Figure S24** – GPC chromatograms for the copolymerisation of VAc, VL, and MDO with **3** (entries 4-6 in Table 2). (A) **P50**, (B) **P100** and (C) **P250**. All chromatograms are normalised to peak height and the dashed line indicates the UV detector trace at 280 nm.

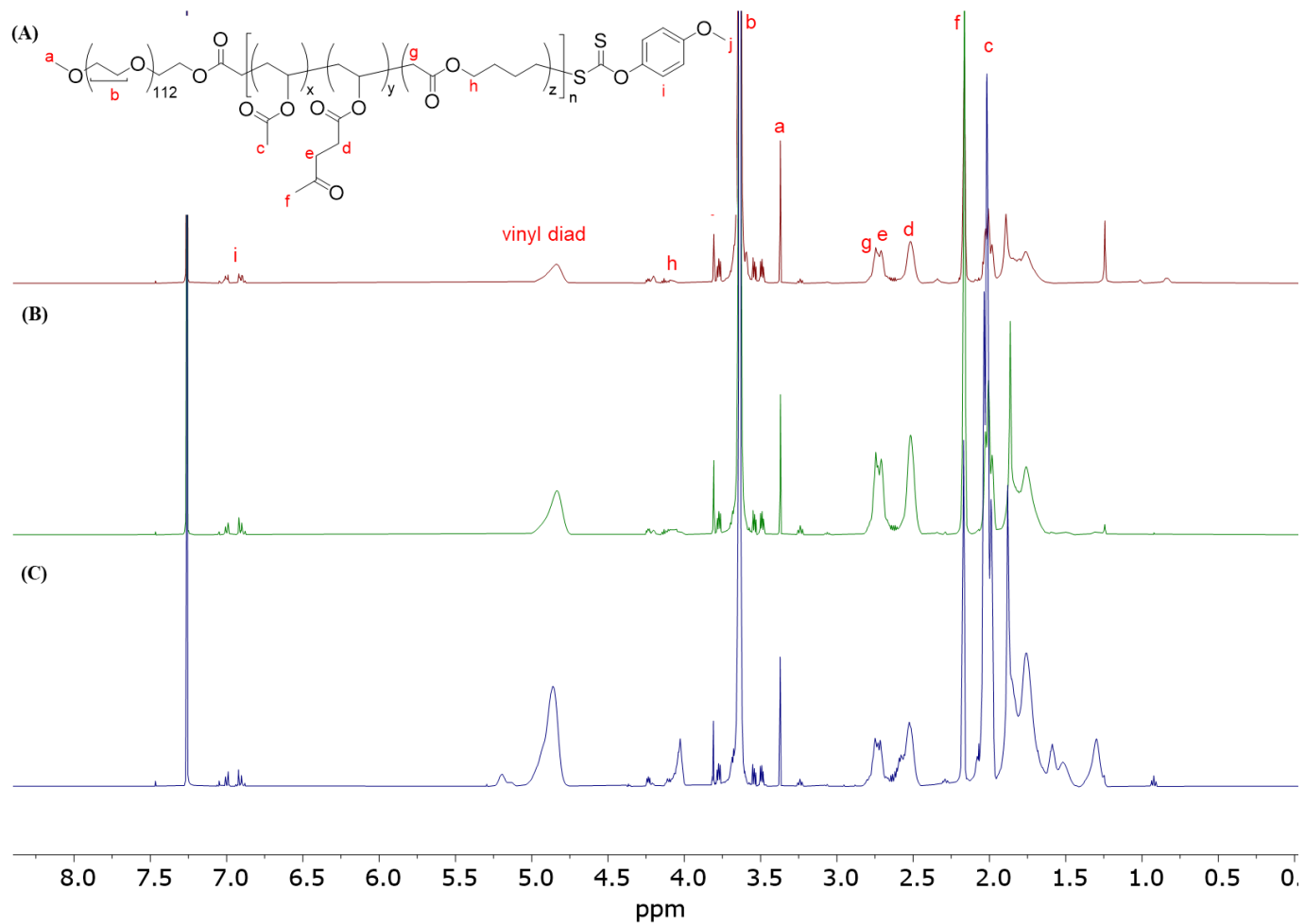


**Figure S25** –  $^1\text{H}$  NMR spectra for the copolymerisation of VAc, VL, and MDO with **3** (entries 4-6 in Table 2). All spectrum intensities are normalised to the PEG signal at 3.6 ppm. (A) **P550**, (B) **P5100** and (C) **P5250**



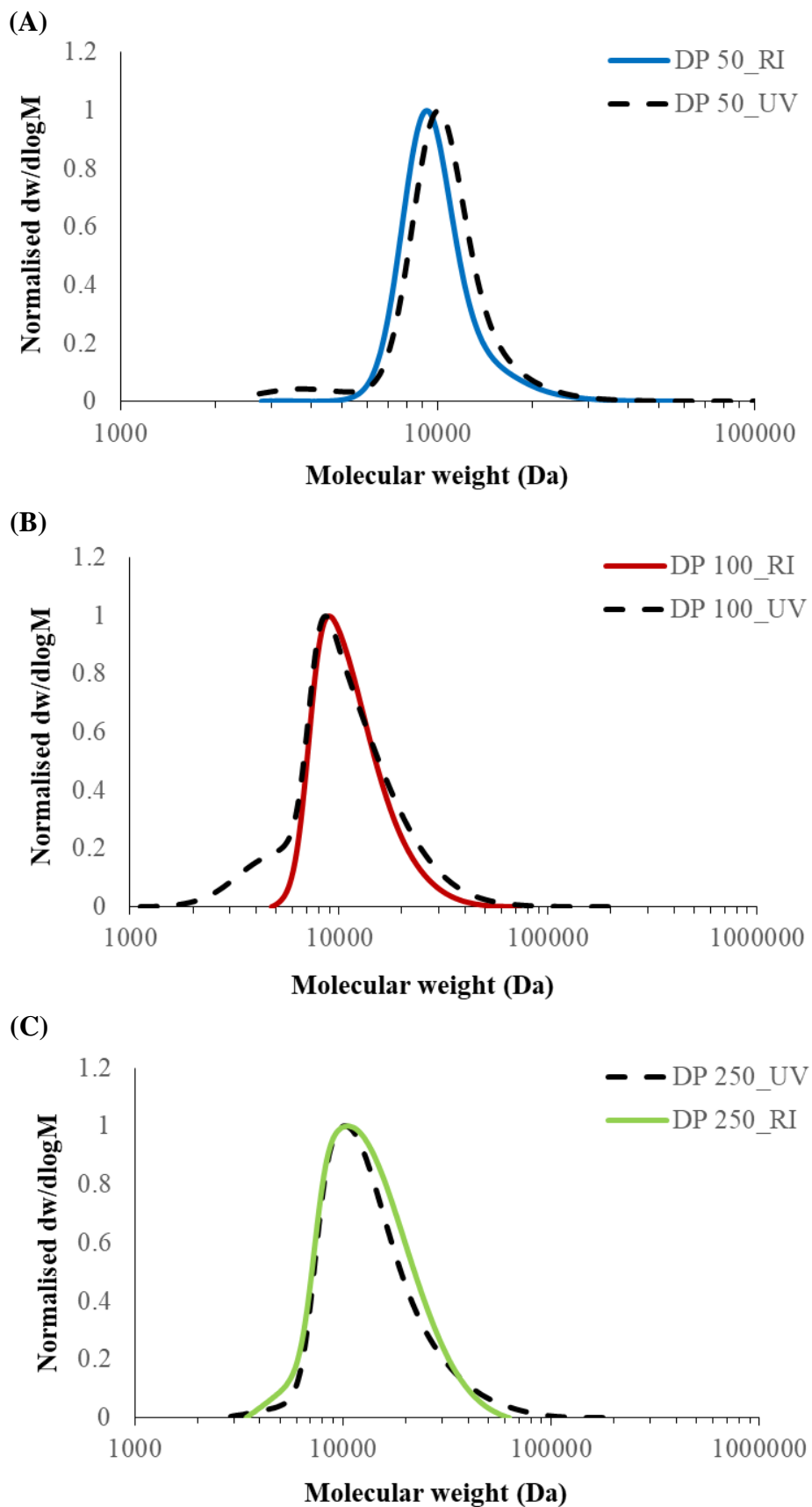


**Figure S26** – GPC chromatograms for the copolymerisation of VL and MDO with **3** (entries 7-9 in Table 2). (A) **P650**, (B) **P6100** and (C) **P6250**. All chromatograms are normalised to peak height and the dashed line indicates the UV detector trace at 280 nm.

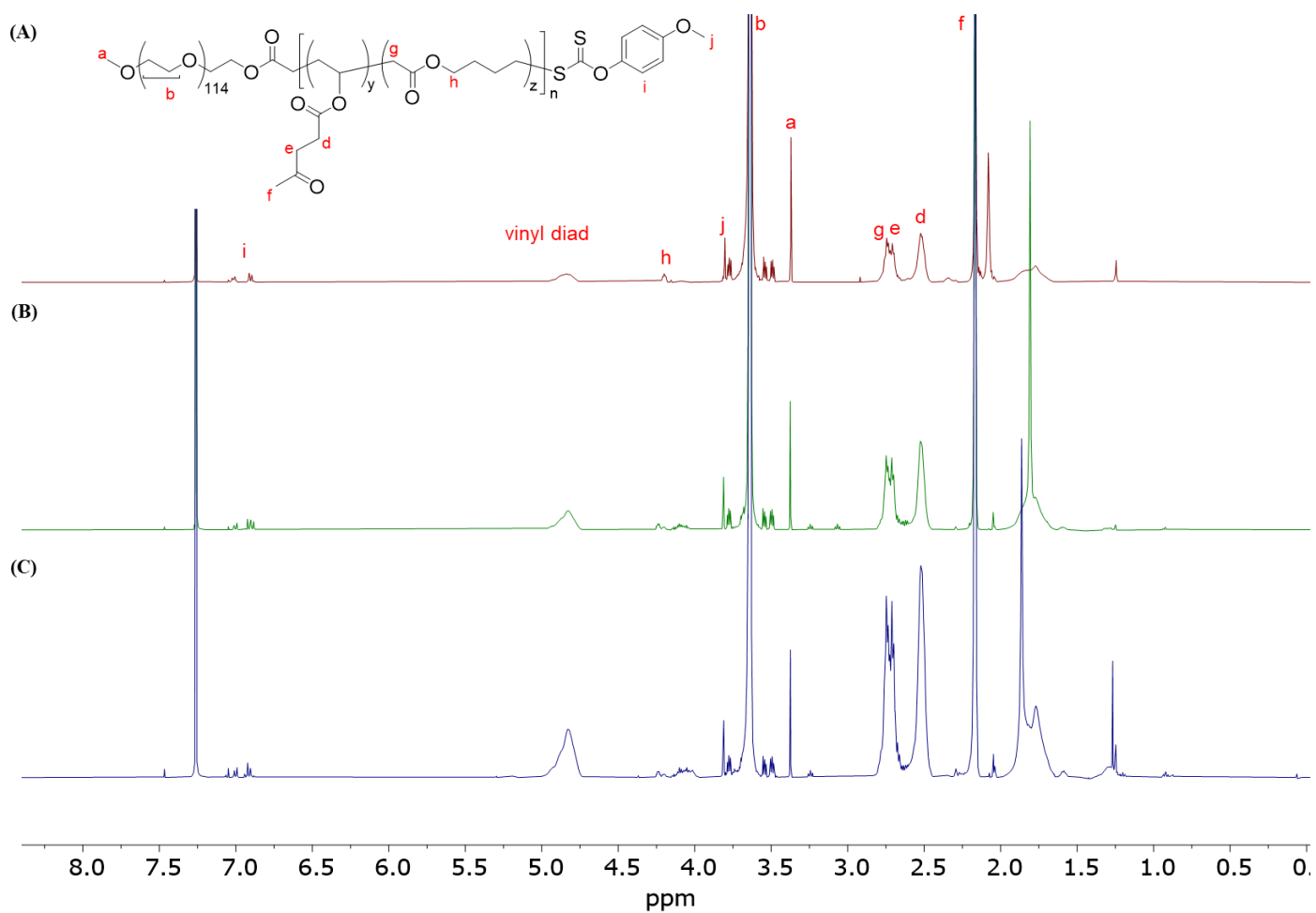


**Figure S27** –  $^1\text{H}$  NMR spectra for the copolymerisation of VAc, VL, and MDO with **3** (entries 7-9 in Table 2). All spectrum intensities are normalised to the PEG signal at 3.6 ppm. (A) **P6<sub>50</sub>**, (B) **P6<sub>100</sub>** and (C) **P6<sub>250</sub>**

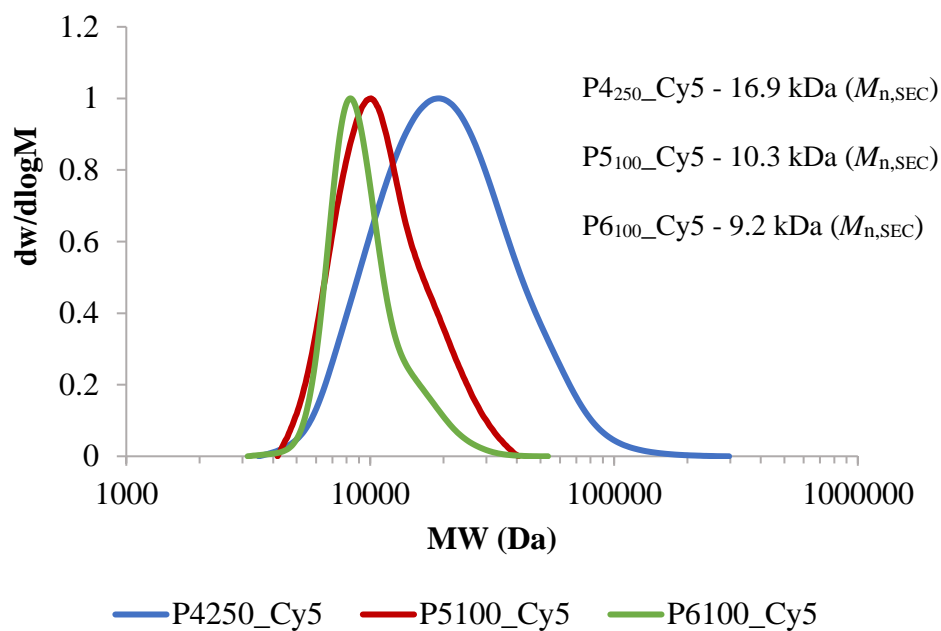


**Figure S28** – GPC chromatograms of the optical dye incorporated version of  $P4_{250}$ ,  $P5_{100}$  and  $P6_{100}$  copolymers (entries in Table 2). All chromatograms are normalised to peak height.

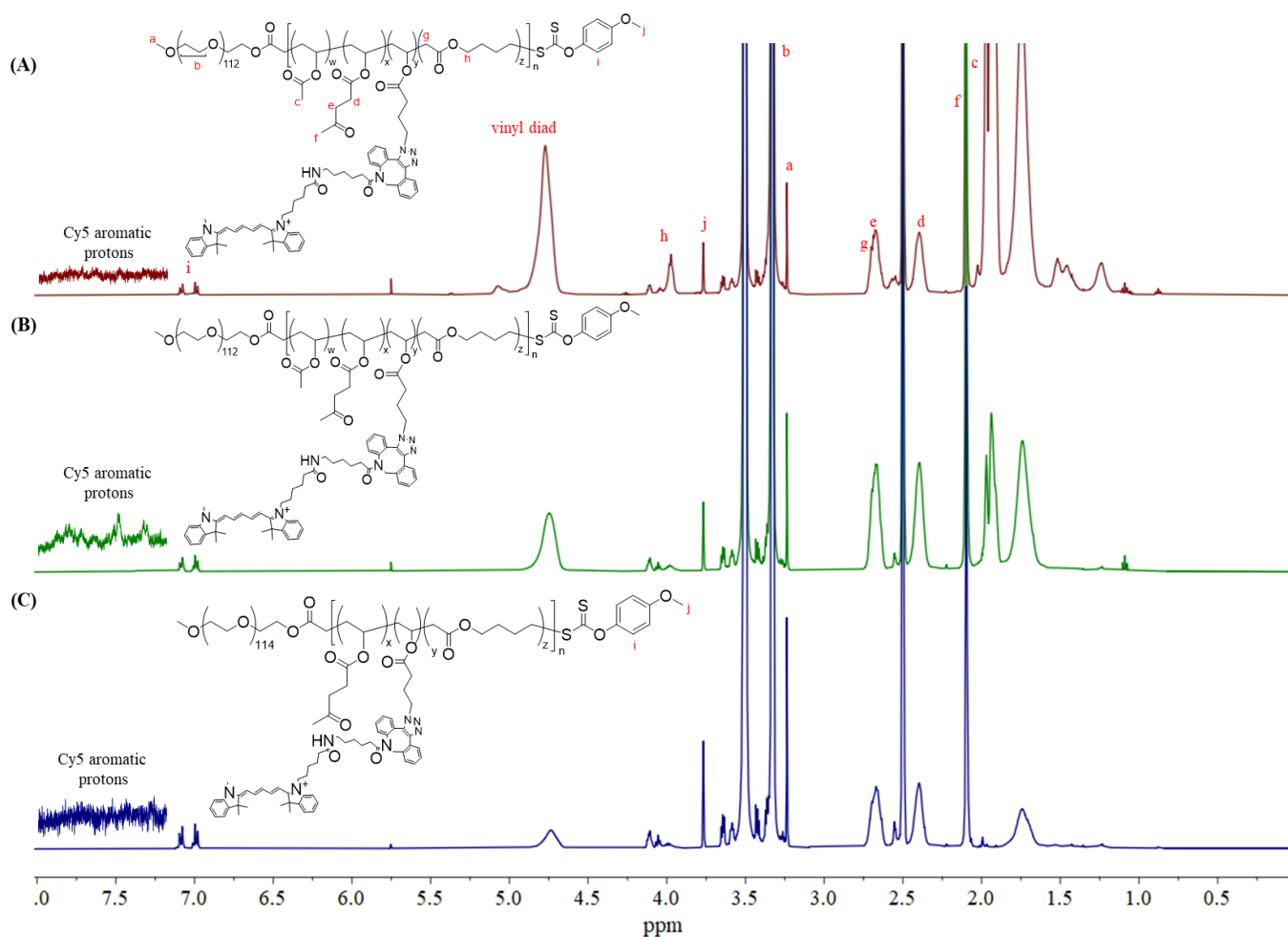


**Figure S29** –  $^1H$  NMR spectra for the optical dye incorporated version of  $P4_{250}$ ,  $P5_{100}$  and  $P6_{100}$  copolymers (entries in Table 2). All spectrum intensities are normalised to the PEG signal at 3.6 ppm. (A)  $P4_{250\_Cy5}$ , (B)  $P5_{100\_Cy5}$  and (C)  $P6_{100\_Cy5}$

## Nanoparticle characterisation

**Table S1**– Nanoparticle size determination of all degradable micelles that have differing crosslink density.

<sup>a</sup> % number distribution; <sup>b</sup> Size determination was averaged from sizing a minimum of 50 micelles; <sup>c</sup> Determined from DLS.

<b>Expt</b>	<b>DLS<sup>a</sup></b> <b>(nm)</b>	<b>TEM<sup>b</sup></b> <b>(nm)</b>	<b>PSD<sup>c</sup></b>
<b>P1<sub>50</sub></b>	18 ± 3		0.24
<b>P1<sub>100</sub></b>	19 ± 3		0.27
<b>P1<sub>250</sub></b>	30 ± 5	28 ± 4	0.19
<b>P2<sub>50</sub></b>	21 ± 3		0.12
<b>P2<sub>100</sub></b>	23 ± 4		0.23
<b>P2<sub>250</sub></b>	32 ± 6	29 ± 4	0.22
<b>P3<sub>50</sub></b>	35 ± 7		0.20
<b>P3<sub>100</sub></b>	33 ± 6	33 ± 5	0.20
<b>P3<sub>250</sub></b>	47 ± 7		0.06
<b>P4<sub>50</sub></b>	16 ± 2		0.20
<b>P4<sub>100</sub></b>	23 ± 1		0.13
<b>P4<sub>250</sub></b>	32 ± 1	26 ± 4	0.12
<b>P5<sub>50</sub></b>	23 ± 2		0.28
<b>P5<sub>100</sub></b>	25 ± 3	23 ± 5	0.40
<b>P5<sub>250</sub></b>	40 ± 2		0.23
<b>P6<sub>50</sub></b>	23 ± 6		0.37
<b>P6<sub>100</sub></b>	30 ± 4	25 ± 6	0.39
<b>P6<sub>250</sub></b>	44 ± 5		0.22

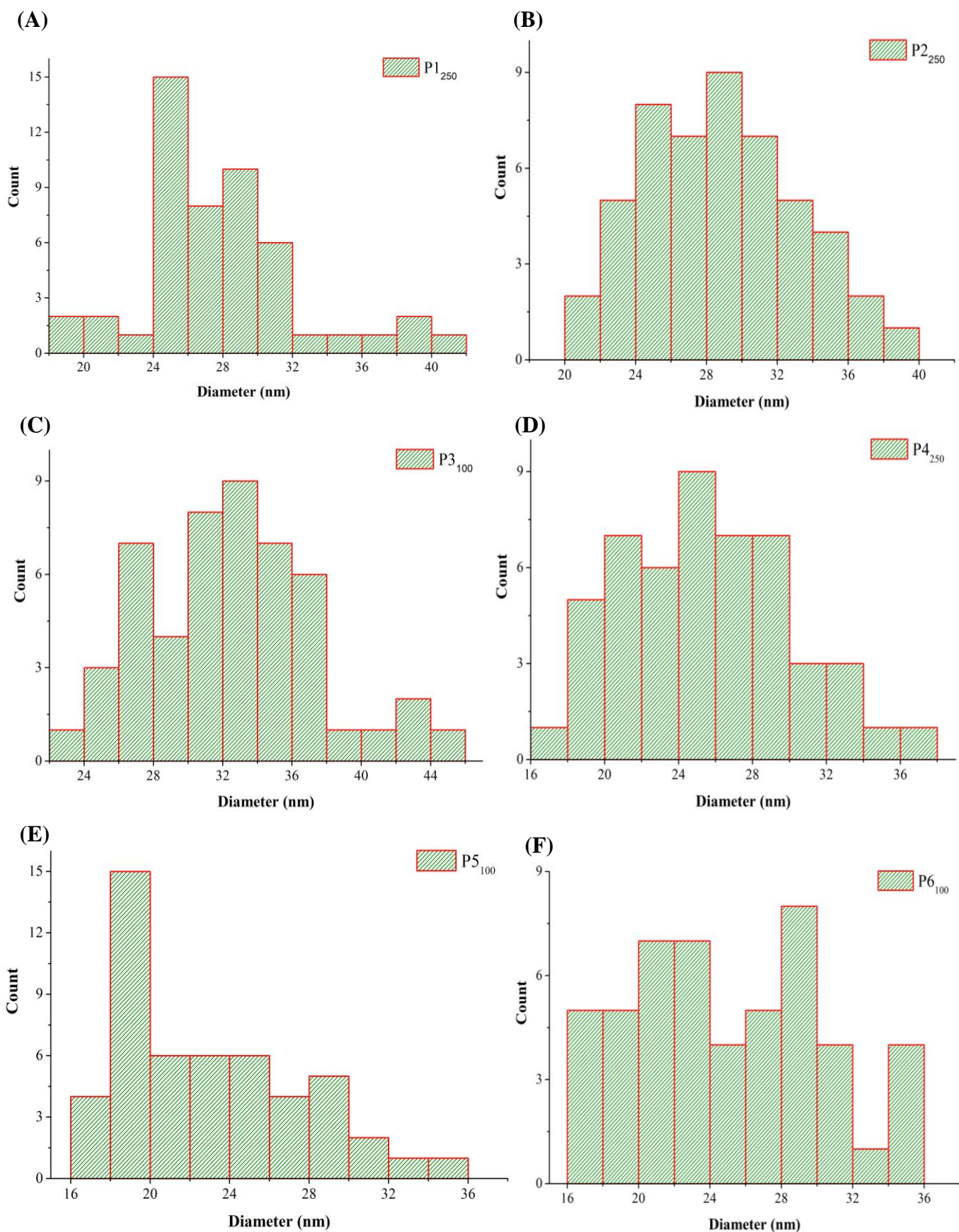


**Figure S30** – Size distribution histograms of SPAAC (A. P1<sub>250</sub>, B. P2<sub>250</sub> and C. P3<sub>100</sub>) and hydrazone (D. P4<sub>250</sub>, E. P5<sub>100</sub> and F. P6<sub>100</sub>) crosslinked polymeric micelles obtained from TEM images.

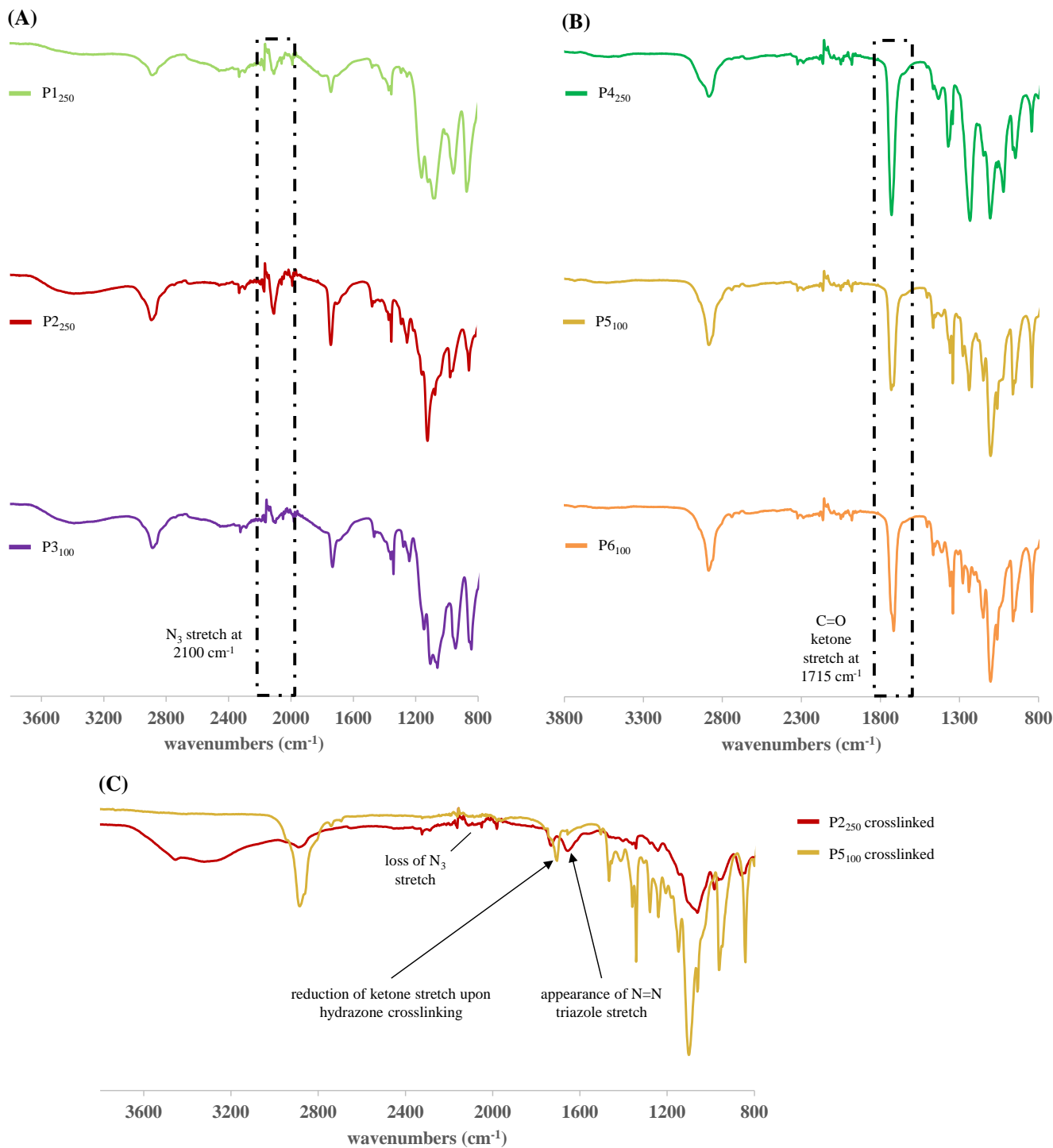


**Figure S31** – ATR-FTIR spectra of biodegradable micelles, (A) Non-crosslinked VN<sub>3</sub> micelles (top to bottom - **P1<sub>250</sub>**, **P2<sub>250</sub>** and **P3<sub>100</sub>**) and (B) Non-crosslinked VL micelles (top to bottom - **P4<sub>250</sub>**, **P5<sub>100</sub>** and **P6<sub>100</sub>**), and (C) Crosslinked micelles via SPAAC (**P2<sub>250</sub>** – **red trace**) showing the loss of N<sub>3</sub> stretch at 2100 cm<sup>-1</sup> and appearance of triazole stretch at 1650 cm<sup>-1</sup>, and hydrazone bond (**P5<sub>100</sub>** – **gold trace**) showing the reduction of ketone stretch at 1715 cm<sup>-1</sup>.

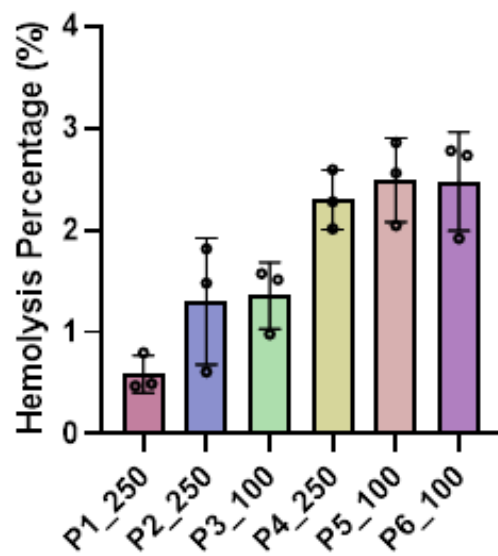


**Figure S32** – Hemolysis percentage of SPAAC and hydrazone crosslinked micelles (600  $\mu\text{g/mL}$  in PBS). Data represented as mean  $\pm$  SD (n=3).

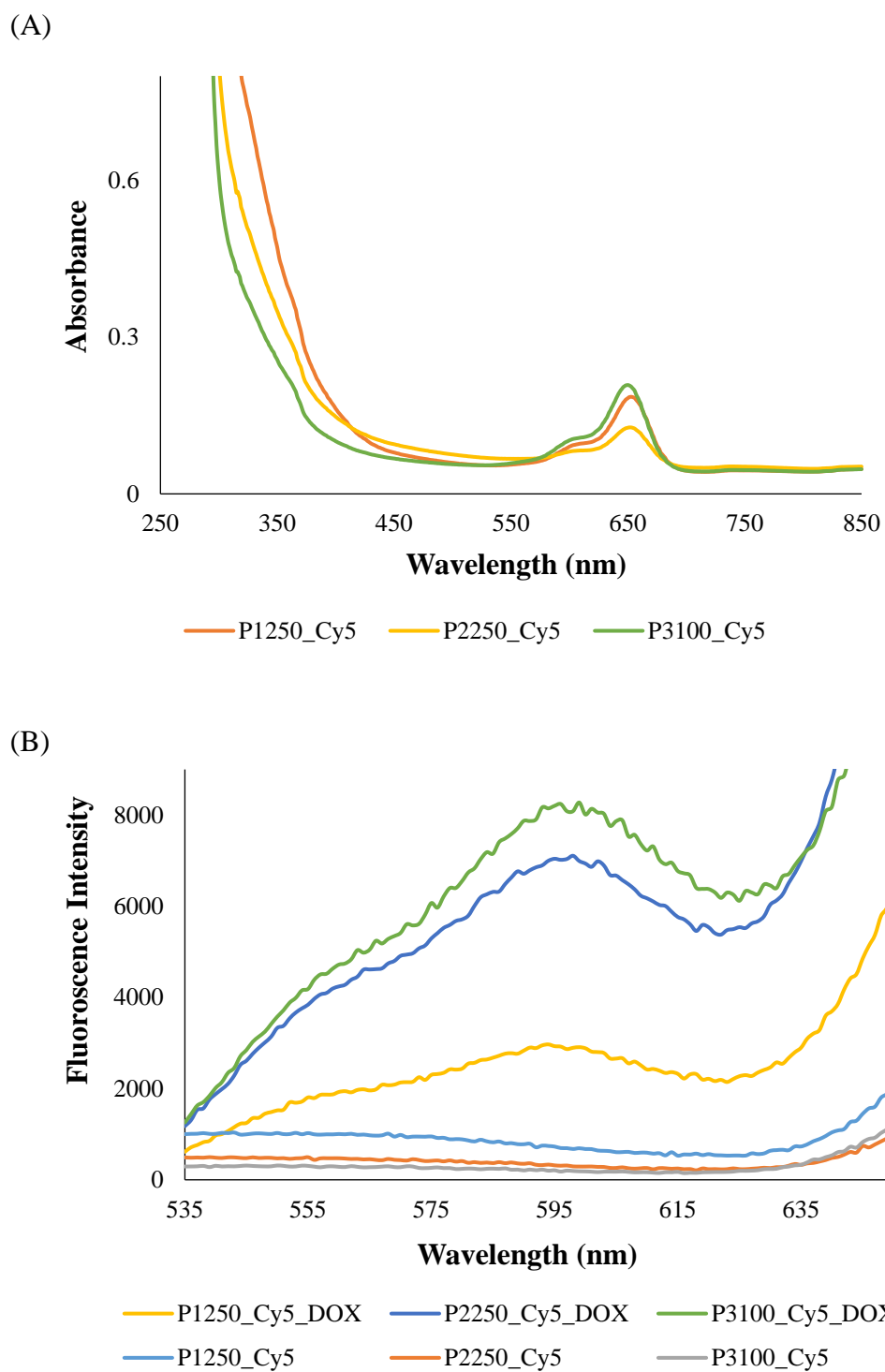


**Figure S33** – (A) UV-vis spectra of SPAAC crosslinked micelles (0.5 mg/mL) of P1<sub>250</sub>-Cy5, P2<sub>250</sub>-Cy5 and P3<sub>100</sub>-Cy5 block copolymers and (B) Fluorescence spectra of SPAAC crosslinked micelles (0.5 mg/mL) of P1<sub>250</sub>-Cy5, P2<sub>250</sub>-Cy5 and P3<sub>100</sub>-Cy5 with and without DOX excited at 488 nm.



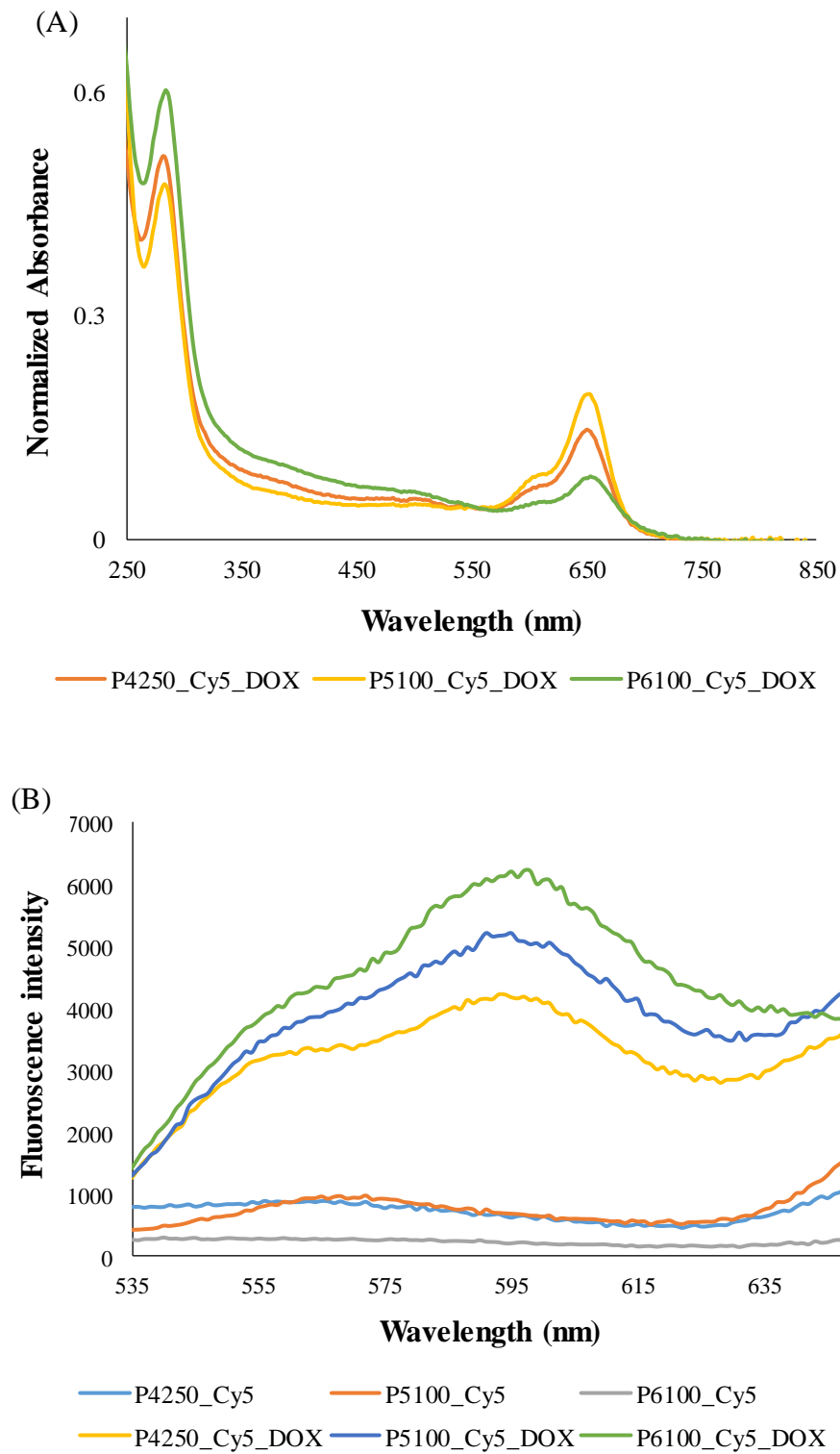


**Figure S34** – (A) UV-vis spectra of DOX loaded hydrazone crosslinked micelles of P4<sub>250</sub>\_Cy5, P5<sub>100</sub>\_Cy5, P6<sub>100</sub>\_Cy5 block copolymers and (B) Fluorescence spectra of hydrazone crosslinked micelles of P4<sub>250</sub>\_Cy5, P5<sub>100</sub>\_Cy5, P6<sub>100</sub>\_Cy5 with and without DOX excited at 488 nm.

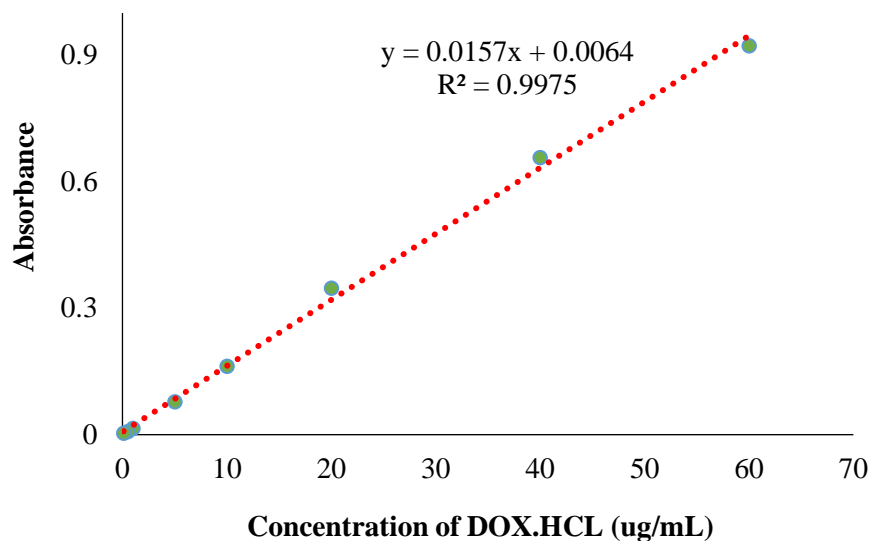


**Figure S35:** Standard curve of DOX.HCl (in PBS) prepared using absorbance values at 498 nm. The drug loading efficiency (DLE) was calculated using the formula,  $DLE (w/w\%) = (\text{Amount of drug loaded (mg/mL)} / \text{Total amount of drug loaded micelles (mg/mL)}) * 100$ .

**Table S2** – Comparison of DLS Z-average and PDI measurements on SPAAC and hydrazone crosslinked micelles after formation (Day 1) and upon storage in 1x PBS (pH 7.4).

<b>Sample</b>	<b>Day</b>	<b>Z-average</b>	<b>PDI</b>
<b>P1<sub>250</sub></b>	1	53	0.16
<b>P2<sub>250</sub></b>	1	57	0.14
<b>P3<sub>100</sub></b>	1	48	0.17
<b>P1<sub>250</sub></b>	22	56	0.20
<b>P2<sub>250</sub></b>	22	54	0.22
<b>P3<sub>100</sub></b>	22	53	0.18
<b>P4<sub>250</sub></b>	1	33	0.26
<b>P5<sub>100</sub></b>	1	46	0.36
<b>P6<sub>100</sub></b>	1	48	0.22
<b>P4<sub>250</sub></b>	6	60	0.72
<b>P5<sub>100</sub></b>	10	85	0.80
<b>P6<sub>100</sub></b>	22	98	0.83

## References

1. A. Balaji, C. A. Bell, Z. H. Houston, K. R. Bridle, B. Genz, N. L. Fletcher, G. A. Ramm and K. J. Thurecht, *Biomaterials*, 2023, **302**.